CHALMERS
UNIVERSITY OF TECHNOLOGY

Development and Implementation of Torque Feedback for Steer-by-wire systems

Master's thesis in Systems, Control & Mechatronics

OSSIAN BERGSTRÖM
JOHAN JANSSON

DEPARTMENT OF MECHANICS AND MARITIME SCIENCES
DIVISION OF VEHICLE ENGINEERING AND AUTONOMOUS SYSTEMS

CHALMERS UNIVERSITY OF TECHNOLOGY
Gothenburg, Sweden 2023
www.chalmers.se

MASTER'S THESIS IN SYSTEMS, CONTROL & MECHATRONICS

Development and Implementation of Torque Feedback for Steer-by-wire systems

OSSIAN BERGSTRÖM
JOHAN JANSSON

Department of Mechanics and Maritime Sciences
Division of Vehicle Engineering and Autonomous Systems
CHALMERS UNIVERSITY OF TECHNOLOGY

Göteborg, Sweden 2023

Development and Implementation of Torque Feedback for Steer-by-wire systems
OSSIAN BERGSTRÖM
JOHAN JANSSON

© OSSIAN BERGSTRÖM, JOHAN JANSSON, 2023

Department of Mechanics and Maritime Sciences
Division of Vehicle Engineering and Autonomous Systems
Chalmers University of Technology
SE-412 96 Göteborg
Sweden
Telephone: +46 (0)31-772 1000

Cover:
The vehicle used for real-time testing of steering feel model.

Chalmers Reproservice
Göteborg, Sweden 2023

Development and Implementation of Torque Feedback for Steer-by-wire systems
Master's thesis in SYSTEMS, CONTROL & MECHATRONICS
OSSIAN BERGSTRÖM
JOHAN JANSSON
Department of Mechanics and Maritime Sciences
Division of Vehicle Engineering and Autonomous Systems
Chalmers University of Technology

Abstract

Steer-by-wire (SbW) has gained significant attention in recent years, revolutionizing vehicle steering by eliminating the mechanical connection between the steering wheel and steering rack. However, by eliminating the connection, the external forces acting on the steering rack are lost and no informative torque feedback will be given to the driver. A solution to this problem is to simulate the corresponding forces by implementing torque feedback using a Force Feedback (FFb) actuator.

The focus of this master's thesis was to develop and implement torque feedback for an SbW system. The objective was to create a steering feel model that simulated a base torque profile and incorporate a set of fundamental features such that the steering feel resembled a conventional steering system with a mechanical connection.

Throughout the thesis, a hardware setup was available, integrated as a testing rig and in a testing vehicle for implementation, testing, and evaluation purposes. The system consisted of a steering wheel, a planetary gearbox, an FFb actuator, an Electronic control unit (ECU), and a steering rack.

A closed-loop model was utilized to simulate the hardware setup in Simulink. The model incorporated the torque input from the driver, FFb actuator, and a reference generator i.e. the steering feel model, and was used for both implementation and testing purposes. After acceptable simulation results, the steering feel model was implemented in the ECU for real-life testing and evaluation of the torque feedback in the testing rig and vehicle.

The initial step of designing the torque profile was by designing the base torque behavior. This was accomplished by deriving a set of system equations based on torque feedback measurements obtained from tests performed on a vehicle equipped with a conventional steering system. The equations contained a set of tunable parameters that were fine-tuned to accurately emulate the measured base torque. Some torque feedback features, such as *End-stop* were subjectively tuned as they were not based on the reference measurements.

The development and implementation resulted in a steering feel model that closely resembled the behavior of the reference steering system, particularly for mid-range vehicle speeds. The steering feel for steering directions away from the center position was found to be satisfactory for all vehicle speeds for real-life testing on the testing rig and in the testing car. However, future work is required to refine the model and achieve hysteresis that fully emulates a conventional steering system for all vehicle speeds. Although, in order to improve the hysteresis, the implementation of a more efficient FFb actuator could minimize the significant influence of the cogging torque in the system. Future work on the features emulating understeer and oversteer is also required.

Overall, this thesis contributed to advancing the understanding and implementation of torque feedback in SbW systems, providing insights for improving the steering feel and driving experience for such systems.

Keywords: Steer-by-wire, Force Feedback, Electric Power Assisted Steering

Acknowledgements

We extend our heartfelt gratitude to Volvo Cars for providing us with an extraordinary opportunity and project that allowed us to showcase and enhance our engineering abilities. It has been an absolute honor to be part of this work.

First and foremost, we would like to express our sincere appreciation to our supervisor, Matthijs Klomp, for his invaluable guidance and support throughout the entire duration of this thesis. His deep interest and passion for the subject matter, combined with his expert guidance, contributed significantly to the quality of our master's thesis.

Our gratitude also extends to our examiner, Fredrick Bruzelius, whose expertise in signal processing and various other subjects greatly enriched our research. We deeply appreciate the insightful conversations and discussions we had with him along the way.

Lastly, we would like to express our thanks to Filip Brink and Linnea Wennberg for their companionship and lighthearted conversations, which brought joy and levity to our days in the office.

We are immensely grateful to everyone mentioned above and to all others who have supported us directly or indirectly during this journey. Without their contributions, this thesis would not have been possible. Their unwavering support, guidance, and camaraderie have been a huge contribution to our success.

Thank you all from the bottom of our hearts.

Nomenclature

Parameters:

τ_{sw} - Torque acting on steering wheel by driver
$\tau_{fricGrd}$ - Torque acting on Steer-by-wire system by tire-ground friction
$\tau_{fricSys}$ - Torque acting on Steer-by-wire system by steering system friction
τ_{FFb} - Torque applied by Force Feedback actuator
J_{FFb} - Moment of inertia of Force Feedback system
b_{FFb} - Damping coefficient of Force Feedback system
$\ddot{\delta}_{sw}$ - Angular acceleration of steering wheel
$\dot{\delta}_{sw}$ - Angular velocity of steering wheel
F_{yf} - Lateral force on front tires
F_{zf} - Normal force on front tires
l - Lever dependent on the contact surface between the tire and the size of the road
τ_a - Aligning torque
t_p - Pneumatic trail
t_m - Mechanical trail
C_f - Front tire cornering stiffness coefficient
α_f - Front tire slip angle
δ - Front wheel steering angle
$\dot{\delta}$ - Front wheel steering angle velocity
δ_{max} - Maximum steering angle before grip starts to decrease
L - Wheel base
R - Turning radius
a_y - Lateral acceleration
v - Vehicle velocity
g - Gravitational acceleration constant
$\mu_{tireGrd}$ - Frictional constant between tire and road
μ_{sys} - Frictional constant for the steering system
k_{sys} - Constant varying the total friction in the steering system
$\sum F$ - Sum of all forces
k - Spring constant
b - Damping constant
$F_{external}$ - External forces acting upon a spring-damper
m - Mass
x - Position
$\dot{x}$ - Velocity
$\ddot{x}$ - Acceleration
τ_{SD} - Torque from spring-damper
y_2 - Base torque second-degree polynomial max torque
x_2 - Base torque second-degree polynomial max torque position
k_2 - Base torque first-degree polynomial slope constant and Base torque second-degree polynomial slope at x_2
m_2 - Base torque first-degree polynomial constant term
$vel_{vehicle\_km}$ - Vehicle speed in km/h
$vehicle_{vel}$ - Vehicle speed in m/s
pos - Current position of the steering wheel
$T_{fricDamp}$ - Friction damping torque
$x_{slipStart}$ - Position at which loss of grip starts
$x_{slipEnd}$ - Position at which grip has been lost
$y_{slipStart}$ - Amount of torque when loss of grip starts
$y_{slipEnd}$ - Amount of torque when grip has been lost
x_{max} - Position at which maximum amount of torque at End-stop has been reached
x_{end} - Position at which End-stop starts
y_{max} - Maximum amount of torque at x_{max}
y_{end} - Amount of torque at which End-stop starts
$b_{baseTrq}$ - Damping variable for On-center damping
$b_{endStop}$ - Damping variable for End-stop

b_{endMax} - Maximum number for $b_{endStop}$
$pos_{shifted}$ - Position shifted from the Displacement of zero torque position
$T_{fricComp}$ - Constant amount of torque used as friction compensation
$T_{integrator}$ - Torque generated by the Return to center integrator
$error$ - Integrator error for the Return to center integrator
K_i - Integrator constant
$T_{integratorMax}$ - Maximum torque that can be generated by the Return to center integrator

Units:
rpm - Revolutions per minute
N - Newton
mNm - Millinewton meter

Acronyms

CAN - Controller Area Network
DC - Direct Current
CAPL - Communication Access Programming Language
RTU - Remote Terminal Unit
ECU - Electronic Control Unit
SbW - Steer-by-wire
FFb - Force Feedback
EPAS - Electronic Powers Assistance System
ECM - Engine Control Module
EBCM - Electronic Brake Control Module
PCM - Powertrain Control Module
VCM - Vehicle Control Module
BCM - Body Control Module
PC - Personal Computer
USB - Universal Serial Bus
LED - Light Emitting Diode
BLDC - Brushless Direct Current

Contents

1 Introduction

Steer-by-Wire (SbW) is a popular topic that is increasing in the automotive industry. A SbW system is a replacement for the mechanical steering system used in most vehicles today. Whereas mechanical steering systems are usually Electric Power Assisted Steering (EPAS) systems. For a SbW system, the mechanical connection between the steering rack and the steering wheel is replaced with an electrical connection. The electrical connection consists of an actuator mounted on the steering rack, a Force Feedback (FFb) actuator mounted on the steering wheel axle, and an Electronic Control Unit (ECU). The actuators include angular sensors to keep track of the position of each actuator.

Removing the mechanical connection results in zero feedback in the steering wheel from all forces acting upon the steering system and disturbances caused by the environment. Hence is the investigation of torque feedback for SbW systems critical to ensure a satisfactory human driving experience. There are different possible methods to achieve satisfactory torque feedback i.e. a satisfactory steering feel. In this project, the torque feedback generation was primarily based on steering wheel torque measurements from a vehicle with an EPAS system.

Since no physical constraints are affecting the connection between the steering wheel and the road wheels, caused by erasing the mechanical connection, the natural safety aspect of having that connection is lost. The overall driving experience might be improved so that the driver can maneuver the vehicle more efficiently over different road conditions and obstacles with a higher probability of preventing driver-inflicted accidents. But it instead exposes the driver to a higher probability of software-inflicted accidents. Therefore, emphasis on safety is essential if the development of Sbw systems is to continue.

One of the advantages of using a Sbw system is that it enables to unconditionally adjust and specify the torque feedback in the steering wheel and the steering ratio between the steering wheel and road wheels. This makes it possible to specifically choose which disturbances should be felt in the steering wheel but also enhance those more important. It also makes it possible to have a steering ratio dependent on the vehicle's speed which is its own topic in itself. Another advantage of Sbw systems is the possibility of designing a new innovative interface that facilitates people with disabilities to make it easier for them to drive vehicles. People who have problems with turning a steering while e.g. parking because of the many degrees a steering wheel might have to be turned might benefit from the possibility of a variable steering ratio that makes it possible to turn the wheels with a smaller steering wheel angle.

1.1 Steering feel background

Steering feel is a complex subject including both subjective and objective components. There are a number of mechanical parts and physicalities playing a role in the composition of a good steering feel. The authors of the paper [14] say that there are two concepts of steering reaction force control i.e. steering feel. Where the first concept is to achieve a steering feel equivalent to an EPAS system where all information from the road and vehicle is transmitted to the driver. The other concept is to make use of the missing mechanical linkage between the steering wheel and the steering rack. This allows for only necessary information to be transmitted to the driver. According to [14] some of the necessary information includes the grip limit of the tires, steering vibrations caused by road surface roughness, contact with obstacles, and full stroke of the steering unit. Some information that could be deemed as unnecessary includes steering wheel movement on a rutted road and steering vibration caused by brake judder. This is all fed back to the driver using an EPAS system.

It can thus be concluded that the steering feel expectations of a SbW system at least includes information regarding the grip limit of tires, steering vibrations caused by road surface roughness, contact with obstacles, and full stroke of the steering unit. Additionally, some information can be filtered out if the missing linkage between the steering wheel and the steering rack is taken advantage of instead of replicating the steering feel of an EPAS system.

In this project, the steering feel from an EPAS system during ideal conditions was used as the base feeling i.e. no additional vibrations were taken into consideration. Then in addition to this EPAS based base steering feel features such as contact with obstacles, full stroke of the steering unit, and grip limit of the tires were developed.

1.2 Problem description

The purpose of this project is to develop a steering feel model for a SbW system that generates a steering feel resembling the feeling of driving with an EPAS system. It is important to note that only the forces acting upon the steering system generated during normal driving conditions with a conventional steering system are to be considered. To accomplish this, a set of features needed to be created to obtain a torque feedback in the steering wheel to imitate the physical forces reacting on the steering rack. The necessary features to be developed and implemented are *Base torque*, *Loss of grip (understeer)*, *End-stop*, *Displacement of zero torque position (oversteer)*, and *Angular velocity limiter*, see section 4 for details on how the features where developed.

- *Base torque*
  The base torque should be the torque felt in the steering wheel created by the forces striving for the steering wheel to be centered. In cars using EPAS the base torque mainly comes from the aligning torque from the tire to road interaction and torque generated from the lateral tire force acting through the caster offset. Therefore should the base torque be inspired by the behavior of the aligning friction torque to generate a steering feel similar to the cars on the road today. This could be done by using the mathematical models for the aligning torque, see section 3. For this project measurement data from an EPAS system was used to develop the base torque.

- *Zero velocity torque*
  The torque profile when the vehicle is stationary should imitate the steering feel of an EPAS system. While stationary, the key distinction is the absence of active return acting on the steering wheel, leading to a displacement of the zero torque position while turning. The zero velocity torque feature should generate a steering feel that closely resembles the steering feel of a vehicle integrated with an EPAS system. This could be achieved by implementing a spring-damper model to generate the torque profile. To serve as a reference, a test was performed to measure the steering wheel torque on a test car, providing a reference torque profile for comparison.

- *Return to center*
  The implementation of an active return feature is a solution to improve the steering feel model. The feature should automatically return the steering wheel to the center position when unhanded. It provides additional torque to assist the base torque, compensating for the combined effects of system friction and the cogging torque generated by the FFb actuator.

- *Loss of traction (understeer)*
  When the grip between the tires and the road starts to decrease the steering wheel torque also starts to decrease. Therefore a feature that decreases the torque when the grip decreases has been implemented. It will be assumed that the friction between the tires and the road is constant while driving. The angle at which the grip starts to decrease is calculated using mathematical correspondences between steering angle and lateral acceleration, see section 3 for details.

- *End-stop*
  For vehicles with a mechanical steering system when turning to the maximal steering angle the steering wheel will stop as well because of the mechanical limitations of the system. It is possible to implement a mechanical end-stop for SbW systems as well but for this project, an electrical end-stop was chosen.

- *Obstacle detection*
  Similarly as for the end-stop for mechanical steering systems, when the tires encounter an obstacle such as a road curb while attempting to turn, the steering wheel will be prevented from turning. Hence, an obstacle detection feature should be implemented to notify the driver when such an event occurs.

- *Displacement of zero torque position (oversteer)*
  If the vehicle starts to skid because of oversteer instead of understeer the zero torque position of the steering system is moved such that it matches the direction of travel of the skidding vehicle. Thus a feature that simulates this behavior is to be implemented. An application of the Displacement of zero torque position could be lane keep assistance.

- *Angular velocity limiter*
  Because of the limitations of the steering rack actuator the steering rack has a maximal traveling speed.

This means that if the steering wheel is turned faster than the steering rack's traveling speed a dynamic mismatch in angle between the steering wheel and road wheels will arise. A feature to retain the synchronization has therefore been attempted to be implemented.

1.3 Limitations

Some limitations have been set for the project to ensure that the focus remains on the project scope.

- External forces not generated during normal driving conditions with a conventional steering system that might affect the general steering feel, will not be considered during the project.
- No other hardware will be used other than the ones implemented on the test rig.
- The software tools used in the project will be limited to CANoe, Simplex Motion Tool, and Matlab.
- Variable steering ratio will not be investigated and is assumed to be implemented.
- A constant road surface will be considered when designing the features.
- The hardware performance of the used prototypes will not be part of the study.

1.4 Related work

Steer-by-wire is a popular subject that has been investigated for a long time for example in the fields of aircrafts and Formula 1 cars. It has only recently reached the production of passenger vehicles with the car company Lexus. There is also previous work regarding the topic of torque feedback for Sbw systems where there have been different methods for generating a satisfying steering feel. For example the research article [8] proposes a control algorithm to create the force feedback for Sbw systems. The authors use a direct current measurement approach to estimate the torque at the steering wheel and at the front axle motor. The authors use this as elements of the feedback torque together with a compensation torque to obtain a realistic feedback torque. To control the feedback torque and vary a steering feel gain the authors use gain scheduling and a Linear Quadratic Regulator (LQR).

Other work related to torque feedback that has taken a different approach is the research article [6] where the authors focus on obtaining driver-environment transparency. Here the authors use a rack force observer to obtain a rack force estimate. This paper does not only investigate transparency for Sbw systems but also EPAS systems where the focus of validation lies on the EPAS system. The authors investigate two different rack-force estimation schemes to find the most reasonable observer that not only gives the best driver-environment transparency but also the best driver-coupled stability. This is due to the closed-loop interconnection that is formed. The advantage of using a rack force estimator is the transparency towards all disturbances affecting the steering rack which means that all forces affecting the steering rack can be felt in the steering wheel.

Previous work related to this project made by the same author as [6] includes the Design of Haptic Feedback Control for Steer-by-Wire [5] and Comparison of Steering Feel Control Strategies in Electric Power Assisted Steering [4].

The paper [5] discusses a comparison of different haptic feedback control strategies where they primarily focus on closed and open-loop methods for FFb SbW systems. It is concluded in this paper that the open loop architecture lacks tracking performance at higher steering excitation frequencies due to feedback motor impedance. However, by using the closed-loop method this impedance is compensated for. Two different control schemes were used with the closed-loop architecture namely position and torque control. By using torque control a higher controller bandwidth was achieved in comparison to position control. By using torque control the closed-loop stability and performance are less sensitive to the driver arm inertia. However, torque control requires filtering of the reference generator which subsequently limits the reference tracking performance. But filtering required on the position controller limits the controller's performance and stability.

The paper [4] instead discusses a comparison between two closed-loop steering feel control concepts i.e. torque control and position control, for EPAS systems. The closed-loop methods aim to compensate the EPAS motor inertia effectively in comparison to an open-loop control scheme. The comparison resulted in the torque control scheme achieving a higher haptic controller bandwidth for reference tracking and stability margin. While the position controller stability and performance are limited due to feedback control filtering

and high system inertia from the EPAS actuator and driver's arms. The torque control scheme offers better road disturbance attenuation for low and high-frequency spectra, while the position control scheme is better in the mid-frequency spectrum.

2 Hardware and software used in Project

The setup of hardware that was available for this project consisted of an ECU from Vector henceforth called the VN module, an integrated servo motor used as a FFb-actuator, a steering rack with an actuator attached, and a steering wheel connected to a planetary gearbox and the FFb-actuator. The VN module was connected through Controller Area Network (CAN) buses with the FFb actuator and the steering rack actuator. All these components together with the necessary power supplies were built into a testing rig that was used as a developing and evaluation tool for the Sbw system.

2.1 Force feedback

The FFb actuator is a servomotor used as a FFb actuator. It is connected to a gearbox which is further connected to the steering wheel.

2.1.1 Actuator

The actuator is an integrated servo motor with a brushless DC outer rotor motor. The actuator has a position and speed encoder utilizing a position sensor measuring 4096 positions for each revolution to estimate the position and speed and an integrated torque estimator that estimated the torque applied. The actuator has two different control modes that were taken into consideration for this project, position control, and torque control. The integrated control electronics make it possible to choose a control mode and a setpoint for that mode through an external source.

Position control

The position control mode for the actuator utilizes an internal tunable PID controller to regulate the position of the motor unit with respect to a setpoint in a closed-loop system, using feedback by increasing the torque of the motor unit. The error of the position is actively calculated as the difference between the setpoint and the process value, i.e. the desired position and the actual position. The control signal is then transformed to the correct voltage and current to increase the torque to reach zero error, where the maximum torque that can be applied is limited by a configurable value.

Torque control

The torque control mode utilizes no internal tunable PID controller, like the position control mode, to regulate the process value. The torque control mode instead uses an unknown controller that cannot be tuned. A torque is assigned as a setpoint and that torque is achieved at the output end of the actuator.

The torque control mode can instead be seen as an open loop system where the torque is assigned without any feedback and transformed to the correct voltage and current to achieve such torque.

Cogging torque

A problem with the actuator motor is something called cogging torque. Cogging torque is a phenomenon that is produced by the magnetic attraction between the rotor-mounted permanent magnets and the stator teeth. Cogging torque is generally seen as a disturbance in the motion of a motor and can cause vibrations and acoustic noise in the motor [13]. There are some techniques to compensate for the cogging torque where one of these techniques, is implemented in the motors electronic control unit as a calibration option. The calibration drastically improves the cogging torque but does not remove it entirely.

There are multiple methods of reducing cogging torque for a BLDC motor and according to [15], three different methods for doing so are possible. The three methods are the following.

- Optimize the air-gap length
- Optimize the rotor structure
- Optimize the stator structure

By increasing the air gap length between the rotor and stator the cogging torque will decrease, the downside is an increase in reluctance torque. Thus, the air gap length must be optimized taking both the cogging torque and the reluctance into consideration.

There are multiple approaches to decreasing the cogging torque by modifying the rotor structure some of them are Magnet pole shaping, Skewing, and lowering the magnet flux density. The more common method is by skewing, either by skewing the magnets or the rotor slots, both have their advantages and disadvantages. According to [15], the cogging torque can in theory be eliminated entirely by optimizing the hardware design. For a real-life implementation, it might not be possible to be erased entirely but reduced significantly.

The structure of the stator can also be optimized and there are 4 different approaches for doing so. Optimizing the thickness of stator tooth tips, the width of the slot opening, the number of slots, and adding an appropriate number of dummy slots. These 4 methods are further described in [15].

In addition, according to [12], the skewing method makes for a complicated production process and therefore increases the construction price significantly.

2.1.2 Gearbox

The gearbox used is a planetary gearbox with a maximum input of 8000rpm and a static gear ratio of 1:9, one rotation of the gearbox shaft is nine rotations of the rotor in the servomotor. The gearbox has a maximum radial load of 265N and a maximum axial load of 220N. Apart from the planetary gearbox, there are other gearboxes that could possibly be utilized for implementation in an SbW system, such as worm gear and belt drive.

The worm gear is a gearbox containing a worm and a worm wheel with their axes perpendicular to one another. There are in general two kinds of worm gears, namely cylindrical and drum-shaped worm gears. According to [17], the advantages of utilizing a worm gear are low noise and low vibration. However, since there is a sliding contact between the worm and the worm wheel they tend to retain heat and has low power transmission efficiency.

Belt drives are constructed of rotating pulleys and a moving belt with corresponding sliding contacts, but there are multiple designs such as V-belt, V-ribbed belts, cog belts, and more. The advantage of using belt drives according to [18], are their cost efficiency and high safety among others. The setback is the endurance of the belt material which over time can lead to fatigue failure and cause a belt to loosen its shape, causing heat to build up from friction due to slippage and bringing damage to the belt.

A gearbox is not a requirement for a SbW system, it was chosen for this particular setup that it was necessary to achieve the correct amount of torque.

2.2 Electronic Control Unit

An Electronic Control Unit (ECU) is in the automotive industry an embedded electronic as described in [7]. Where the ECU basically is a digital computer that reads signals from sensors placed around the vehicle and in certain components in the vehicle. The ECU, then depending on the signals, controls certain units of the vehicle, e.g. the engine, power assistance actuator, and other actuators. There are different types of ECUs in a vehicle depending on which area of the vehicle the controls are actuated.

For this particular project, controls, and monitoring of units that would be under the categorization of VCM are to be considered. Where the ECU to be used for this project is the VN8911 from VECTOR.

2.2.1 Vector VN8911

The VN8911 is one of the base modules of the 8900 interface family and the base module used for the steer-by-wire system used in this project. VN8911 is an ECU specifically designed for high-performance applications using CANoe and CANalyzer [16]. An important characteristic of the VN8911 is the modularity of the network interface i.e. the communication ports. The complete system composes of one base module (the processor unit) and one plug-in module, which represents the network interface. For this particular system setup, the VN8970 is used as the plug-in module. To configure the VN8911 the software tool CANoe, see section 2.2.3 for details on CANoe, is used. The module is configured through a Personal Computer (PC) connected via Universal Serial Bus (USB) to the module and the configuration is executed inside the module itself. See figure 2.1 for the module used in the project.

Figure 2.1: *Image of the VN8911 with VN8970 plug-in module*

2.2.2 CANoe

CANoe is a flexible software tool from VECTOR for the development, analysis, and testing of individual ECUs and complete ECU networks [1]. This tool is used to be able to implement torque feedback solutions in the ECU for real-world testing. It is needed to set up simulated ECUs, system variables, write code, analyze measurements, and operate the system.

2.2.3 Communication Access Programming Language (CAPL)

Communication Access Programming Language (CAPL) is a procedural programming language developed by VECTOR that is similar to C [3]. The programming language is event-based and CAPL programs are developed and compiled in a dedicated browser. Because of this, it is possible to access all objects contained in the dataset e.g. messages, signals, environment variables, and system variables.

2.3 Steering rack

The steering rack used for this project was a steering rack mounted in a Volvo V60 2019. The internals of a steering rack that moves consist of a gear rack that moves from side to side when turning the steering wheel which turns the road wheels. The gear rack is moved by a gear called a pinion which rotates with the steering wheel which in turn moves the gear rack, see figure 2.2. For a conventional mechanical steering system e.g. EPAS the steering wheel is mechanically connected to the pinion by the steering column but for Sbw systems the pinion is connected to the steering rack actuator, see figure 2.3 for a mechanical steering system.

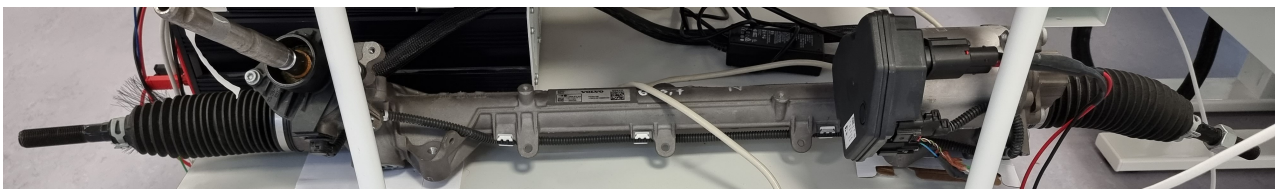

Figure 2.2: *An image of the steering rack used in the project*

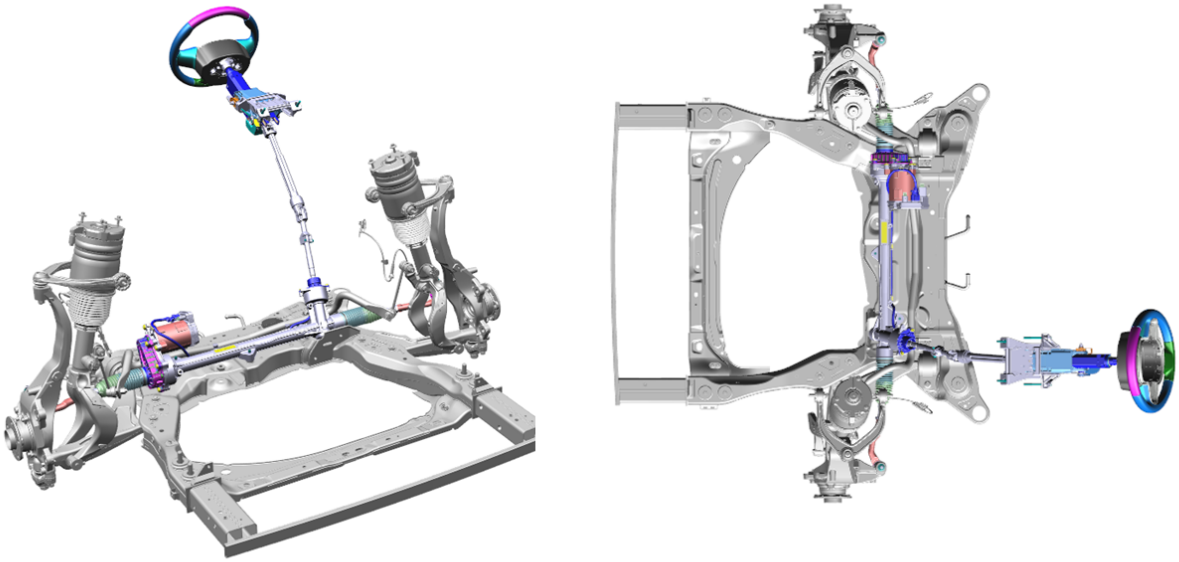

Figure 2.3: *Visualization of the complete mechanical steering system used in the testing vehicle.*

2.4 Testing rig

The complete testing rig used in the project consisted of a steering wheel connected to the gearbox with an assumed to be rigid axle which is coupled with the FFb actuator. The FFb actuator is connected via a CAN-bus to the ECU and is powered by a power supply. The steering rack actuator was connected via CAN-bus to the ECU as well. The ECU was also connected to a control box with some switches and Light Emitting Diodes (LEDs) that were used as a simple communication interface with the operator to e.g. start the torque feedback, let the operator know that the feedback is active or change steering ratio. The ECU was also connected with USB to a PC to be able to operate and modify the software of the testing rig.

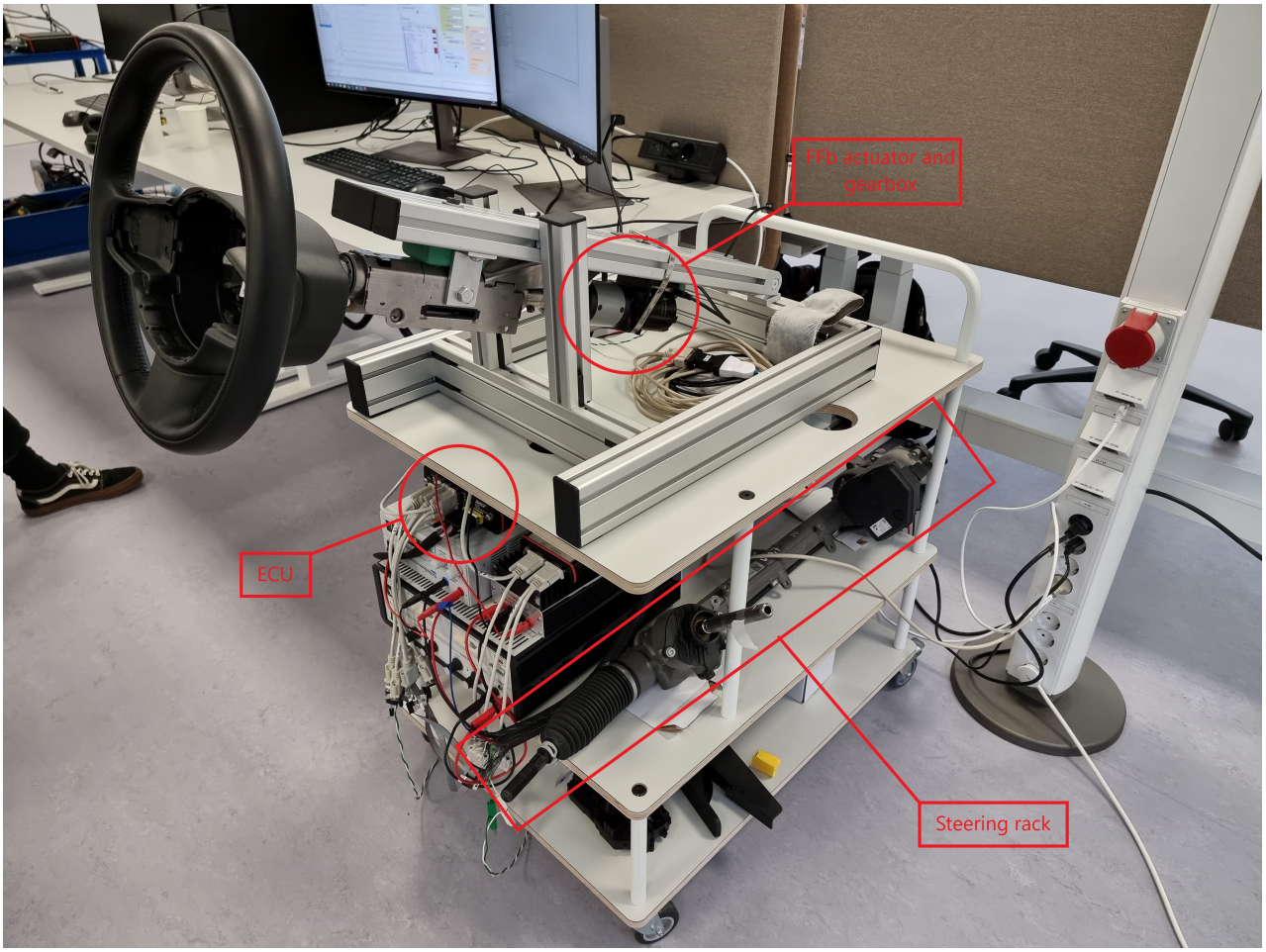

Figure 2.4: *The testing rig with the steering wheel, FFb actuator, ECU, and steering rack.*

2.5 Developing and Implementation software

For the developing phase and early evaluation of the features, mainly Matlab and Simulink were used. While for the implementation phase and final evaluation of the steering feel model, CANoe was used.

2.5.1 Matlab

Matlab is a powerful programming platform allowing for an effective way of solving computational mathematics e.g. matrix-based multiplication and design systems. It was utilized to derive the torque feedback algorithms and to evaluate the results by analyzing corresponding plots. Matlab was the primary platform used in the development and simulation phase of the project before the real-life implementation of the model was realized. Doing so prevented unnecessary wear and tear on the testing rig hardware and provided a safe testing environment if unintended torque values were to be generated. Matlab was used to design all individual torque curves for each feature composing the steering feel model except the zero velocity torque feature and the damping around the center position and End-stop. The torque curves developed in Matlab were generated by defining each curve with an equation system consisting of tunable parameters and then solving the equations system giving the solution to each curve parameter as functions of tunable parameters.

2.5.2 Simulink

Simulink is a powerful tool often utilized to simulate, analyze, and verify model-based systems. During this project, it was used as a tool to build a simple mathematical model of the real-life testing rig available and run simulations of the functions developed in Matlab before real-time implementation. Since the FFb actuator

has the ability to generate high torque values, implementing and verifying the results in Simulink beforehand prevented possible unnecessary damage to the hardware as well as the driver. The following figure illustrates the simulation setup in Simulink and the different components.

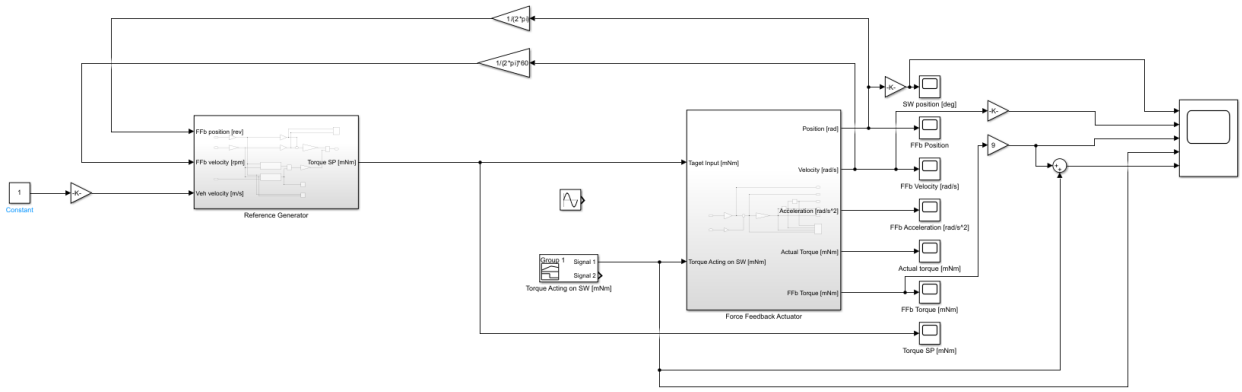

Figure 2.5: *Image illustrating the simulation setup in Simulink,*

The main components of the simulation setup are the Reference Generator, Force Feedback Actuator, and torque input from the steering wheel. The setup is a closed-loop direct feedback model that represents the testing rig and communication between the VN-module, steering rack, and FFb actuator. The reference generator represents the torque feedback model taking the FFb motor position and angular velocity for each loop as well as the vehicle speed as inputs. The reference generator generates a torque feedback set-point which is directly transmitted to the FFb actuator block. The steering wheel torque input is symbolizing the driver steering torque input. The steering wheel torque input and the set-point act as the inputs to the FFb actuator. The FFb actuator computes the torque difference between the reference torque and the driver steering torque and transmits the current FFb motor position and angular velocity back to the reference generator, forming a closed-loop model.

2.5.3 CANoe

CANoe is the software used in the VN-module for implementation and evaluation as described in section 2.2.2. During the development phase, parts of the steering feel model were implemented using CANoe. This was to ensure that the features performed correctly before the whole steering feel model was to be implemented and evaluated. The complete features required to be converted from Matlab syntax to CAPL for it to work in CANoe. During the evaluation of the features, a number of variables such as estimated FFb actuator torque, FFb actuator position, FFb actuator angle speed, pinion angle, pinion angle speed, and reference torque were logged and analyzed.

3 Modelling of Steering system

Before starting the implementation on the physical system some simulations in Simulink need to be performed to ensure that e.g. the correct torque is generated at the correct position and speed. This requires a simple model of the physical system which is discussed in this section. It is also important to note that the torque feedback that occurs in the steering wheel in a vehicle with a mechanical steering connection, e.g. EPAS, comes from actual physicalities in the system. How these occur and can be modeled are also briefly discussed in this section to clarify where the torque feedback in the steering wheel comes from.

3.1 Steer-by-wire system

The SbW system consists of two smaller systems, the FFb system, and the steering rack system. The FFb system consists of a steering wheel connected to the planetary gearbox by a, assumed to be rigid, solid axle. The planetary gearbox is directly connected with the FFb actuator with a short rigid axle, see figure 3.1.

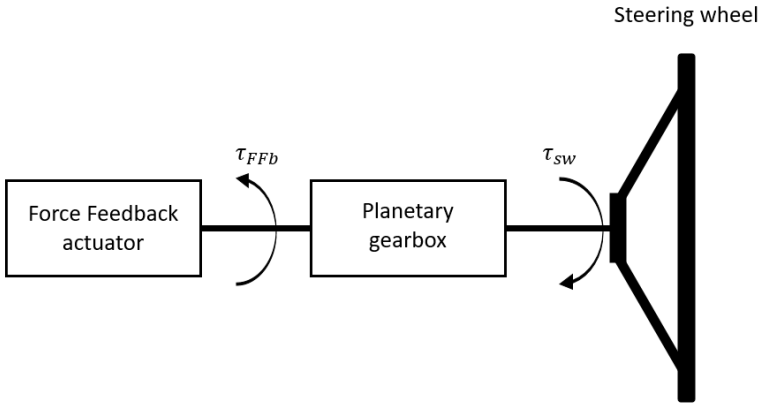

Figure 3.1: *Force feedback system*

The FFb system can be simplified to be described as the following model

$$\tau_{sw} = \tau_{FFb} + \tau_f + J_{FFb}\ddot{\delta}_{sw} + b_{FFb}\dot{\delta}_{sw} \tag{3.1}$$

where τ_{sw} is the torque acting on the steering wheel given by the driver, τ_{FFb} is the torque from the FFb actuator, τ_f is the torque created by the friction in the system (assumed to be constant), J_{FFb} is the moment of inertia of the system, b_{FFb} is the damping coefficient of the system, $\ddot{\delta}_{sw}$ is the angular acceleration of the steering wheel and $\dot{\delta}_{sw}$ is the angular velocity of the steering wheel.

The steering rack system consists of a steering rack rigidly connected to an actuator via a pinion, see figure 3.2.

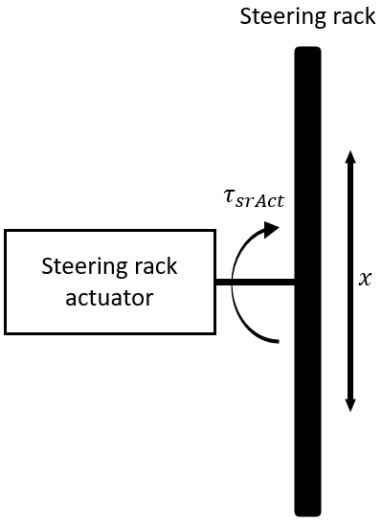

Figure 3.2: *Steering rack system*

It is known that the maximum angle of the pinion is 9rad and the maximum pinion angle speed by the steering rack actuator is 6rad/s.

3.2 Aligning torque

One of the largest components of the steering feel is the aligning torque τ_a generated while cornering i.e. turning the steering wheel. When the velocity of the tire is not in the same direction as the tire is pointing, i.e. slipping is occurring, a lateral force F_{yf}, a pneumatic trail t_p, and a mechanical trail t_m are generated. The aligning torque can be modeled as the following equation

$$\tau_a = F_{yf}(t_p + t_m) \tag{3.2}$$

where the pneumatic trail is the distance between the center of the tire contact patch and the point where the lateral force is acting and the mechanical trail is the distance between the center of the tire and the point where the steering axis intersects the ground, see figure 3.3. The lateral force can be modeled as the following equation

$$F_{yf} = 2C_f\alpha_f \tag{3.3}$$

where C_f is the front tire cornering stiffness coefficient and α_f is the slip angle of the front tires. The cornering stiffness is a constant depending on the tire and the slip angle is the angle between the direction of travel and the direction of the tires that is e.g. dependent on the grip between the tires and the road, and the velocity of the vehicle [9].

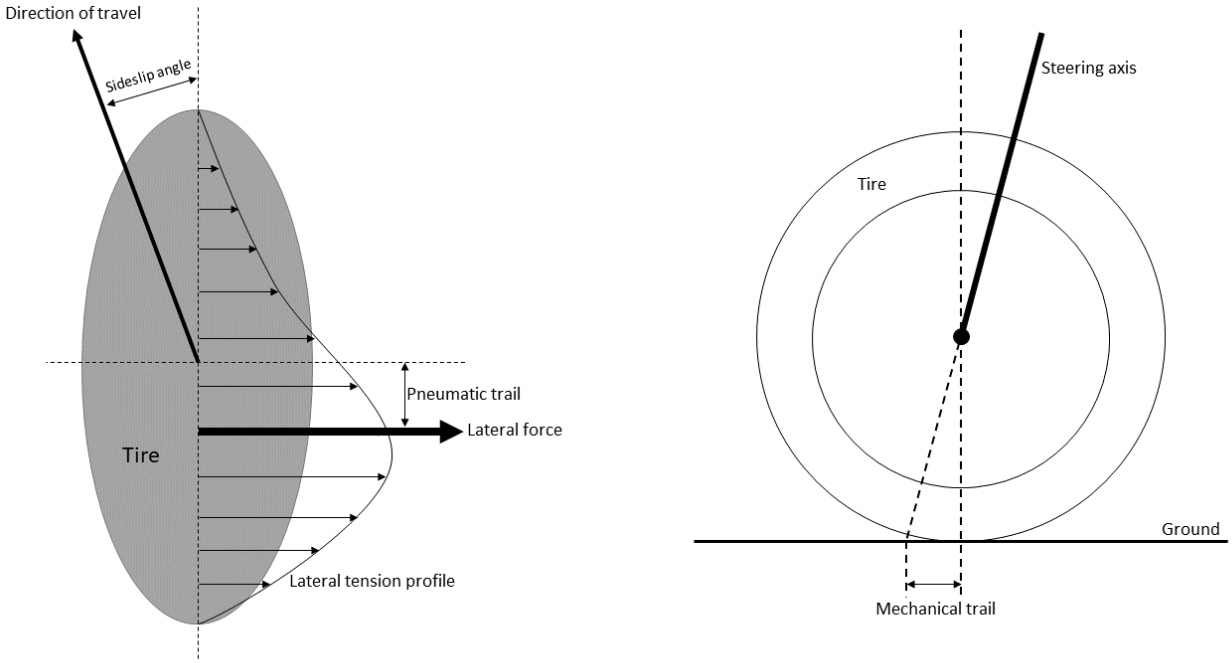

Figure 3.3: *Visualization of pneumatic trail and mechanical trail.*

3.3 Friction torque

Another significant contribution to the steering feel is the frictional torque generated by the mechanical friction affecting the system. One component of the mechanical friction is the friction between the road and tires $\tau_{fricGrd}$. Where the frictional torque can be modeled as

$$\tau_{fricGrd} = F_{zf}\mu_{tireGrd}sign(\dot{\delta})l \tag{3.4}$$

where F_{zf} is the normal force generated by the front tires, $\mu_{tireGrd}$ is the friction coefficient, $\dot{\delta}$ is the angular velocity of the front tires, and l is a lever dependent on the contact surface between the tire and the size of the road. The friction torque affected by the friction between the tires and the road is only significant when the vehicle is stationary or operating at very low speeds. Another component of the total mechanical friction is the friction within the steering system $\tau_{fricSys}$. This can be modeled as

$$\tau_{fricSys} = k_{sys}\mu_{sys}sign(\dot{\delta}) \tag{3.5}$$

where μ_{sys} is the frictional constant of the steering system and k_{sys} is a constant that scales the total frictional torque within the steering system. The steering system friction affects the steering feel independent of the vehicle speed. However, when the vehicle is stationary or operating at very low speeds the frictional torque between the tires and the road is the dominant part of the total mechanical friction.

3.4 Spring-damper

The mass-spring-damper model is a common model used as a simplification to model different physicalities e.g. tires, in this project different interpretations of the mass-spring-damper model have been used to generate the force feedback torque. Where the typical linear mass-spring-damper model can be derived as the sum of all forces acting upon the system as

$$\sum F = -kx - b\dot{x} + F_{external} = m\ddot{x} \tag{3.6}$$

where $\sum F$ is the sum of all forces, k is the spring constant, b is the damping constant, $F_{external}$ are the external forces acting upon the system, m is the mass, x is the position of the spring, $\dot{x}$ is the velocity of the spring and $\ddot{x}$ is the acceleration of the spring.

In this project, the linear spring-damper model looks like

$$\tau_{SD} = -kx - b\dot{x} \tag{3.7}$$

where τ_{SD} is the torque that will be applied because of the spring-damper model. A nonlinear spring-damper model used in this project looks like

$$\tau_{SD} = -kx^2 - b\dot{x}^2. \tag{3.8}$$

In some cases, the damping constant might also be dependent on the position, i.e. the value of b changes with x.

3.5 Loss of grip from understeer

Understeer is what happens when the vehicle steers less than the steering angle. This happens when the slip angle gets to large i.e the lateral force gets to large. For there to be a lateral force on a point mass a lateral acceleration a_y has to exist and the acceleration of the point mass can be estimated as

$$a_y = \frac{v^2}{R} \tag{3.9}$$

where v is the velocity of the vehicle and R is the turning radius. The steering angle δ can be estimated as

$$\delta = \frac{L}{R} \tag{3.10}$$

where L is the wheelbase of the vehicle. Inserting equation 3.9 into equation 3.10 then gives

$$\delta = \frac{a_y L}{v^2} \tag{3.11}$$

where the maximum lateral acceleration that can be reached before losing grip can be approximated to μg. This gives a maximum steering angle for when the vehicle starts losing grip as

$$\delta_{max} = \frac{\mu g L}{v^2} \tag{3.12}$$

where μ is the frictional constant between the tire and the road, and g is the gravitational acceleration constant. If the aligning torque is then plotted against the slip angle, see e.g [2], it can be seen that the slip angle for when the maximum aligning torque has been reached is approximately 40% of the slip angle when all grip has been lost i.e the aligning torque has decreased to zero. It is thus also assumed that for all vehicle velocities, the aligning torque is zero at $1.5\delta_{max}$.

4 Development and Implementation of Torque Feedback

This chapter presents the implementation of the developed solutions of the steering feel model. The first section describes the software tools used for the development and implementation of the solution and the rest of the chapter describes each feature composing the steering feel model. The hardware presented in section 2 was used throughout the project, hence, the model is designed and tuned thereafter. The torque profile generated by the steering feel model is based on the reference pinion angle, where the reference pinion angle is computed from the steering wheel angle and the steering ratio such that the torque profile always remains identical independent of the steering ratio. The steering ratio used during this project was 1:1 such that the steering wheel angle is equivalent to the reference pinion angle at all times.

4.1 Base torque

The base torque feature provides a multivariable nonlinear base torque curve dependent on the vehicle speed, pinion angle, and pinion angular velocity where the active range of the base torque feature generates an output for all vehicle speeds greater than 0m/s. The complete base torque profile is designed as a spline containing a first-degree polynomial $y = k_2x + m_2$ that is a continuation of a second-degree polynomial $y = a_1x^2 + b_1x + c_1$ added together with a hyperbolic tangent function (Tanh) to replicate a similar torque curve based on measurements from an EPAS system instead of physical models. To attain the desired characteristics of the base torque slope, an equation system was defined for the second-degree polynomial to be symbolically solved to obtain the functions for the polynomial parameters. The equation system was defined as

$$y_2 = a_1x_2^2 + b_1x_2 + c_1 \tag{4.1a}$$

$$k_2 = 2a_1x_2 + b_1 \tag{4.1b}$$

$$0 = c_1 \tag{4.1c}$$

where it is defined that the second-degree polynomial intersects the origin, the torque at x_2 is y_2 and the gradient at x_2 is k_2 where x_2 is the angle at which the base torque curve transforms from the second-degree to the first-degree polynomial. Solving the equation system gave the following functions for the second-degree polynomial parameters

$$a_1 = -\frac{y_2 - k_2x_2}{x_2^2} \tag{4.2a}$$

$$b_1 = \frac{2y_2 - k_2x_2}{x_2} \tag{4.2b}$$

$$c_1 = 0. \tag{4.2c}$$

The first-degree polynomial continues with the gradient k_2 and the parameter m_2 is calculated as

$$m_2 = a_1x_2^2 + b_1x_2 + c_1 - k_2x_2. \tag{4.3}$$

The tuning parameters y_2 and k_2 are then calculated as the following

$$y_2 = -0.0633vel_{vehicle\_km}^2 + 44.1664vel_{vehicle\_km} + 400.0816 \tag{4.4a}$$

$$k_2 = 0.0680vel_{vehicle\_km}^2 + 18.1468vel_{vehicle\_km} \tag{4.4b}$$

where $vel_{vehicle\_km}$ is the driving speed of the vehicle in km/h. Equations 4.4 were found from curve-fitting data from the EPAS measurements for different vehicle speeds at the same pinion angle using second-degree polynomials. The torque values at 0.5 rad pinion angle for the vehicle speeds 30km/h, 45km/h, 60km/h, 80km/h, and 100km/h were used together with the Matlab function *Polyfit()* to find and approximating second-degree polynomial function describing the torque at 0.5rad pinion angle for all vehicle speeds i.e. equation 4.4a. The same torque values were also subtracted to a torque value for one larger pinion angle for each vehicle speed and divided by the difference between the two pinion angles to get a function that approximately describes the gradient of the first-degree polynomial torque curve for all vehicle speeds i.e. equation 4.4b. By utilizing these

polynomial equations, a base torque profile is generated that always intersects the origin while steering passed the center position.

Additionally, the torque curves of the base torque profile are designed to be combined with a Tanh function that can be seen as a frictional damping of the physical system [11]. By observing e.g. the EPAS measurements in figure 6.2, a hysteresis can clearly be noted which was considered to be a frictional damping of the physical system. This hysteresis was replicated using the Tanh function as a function of pinion angular velocity since the hysteresis seemed to have a maximum limit of approximately 1Nm. The Tanh function affects the base torque profile by smoothly adding an additional 1000mNm of torque to the base torque profile when the pinion angular velocity is non-zero. However, if the pinion angular velocity is zero, the Tanh function smoothly transitions to adding 0mNm to the base torque profile. The following equation defines the Tanh function used to replicate the hysteresis

$$T_{fricDamp} = \frac{e^{a \cdot x} - 1}{e^{a \cdot x} + 1} \cdot 1000 \tag{4.5a}$$

where $T_{fricDamp}$ is the additional torque generated by the Tanh function, a is the gradient of the Tanh function at origin and x in this case represents the pinion angular velocity. The characteristic of a Tanh function can be seen in figure 4.1 below.

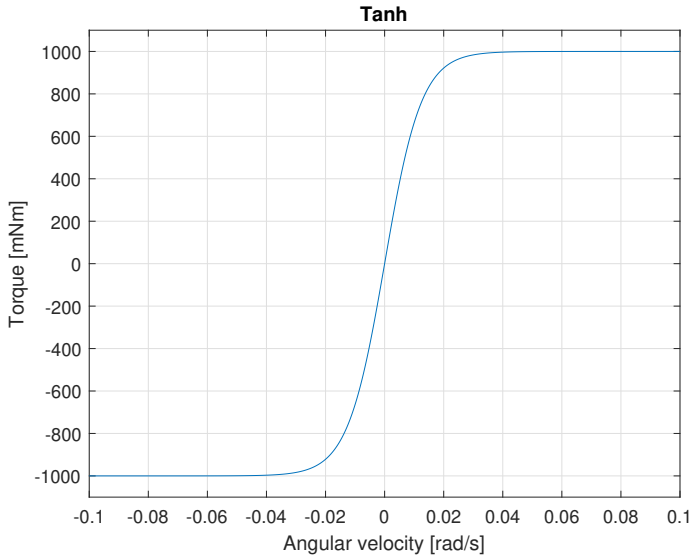

Figure 4.1: *An illustration of the Tanh function i.e. the hysteresis added to the torque curves generating the complete base torque profile.*

The complete base torque profile can be visualized as figure 4.2 if the steering wheel would start as stationary at 0rad and linearly increase the pinion angular velocity to 3rad/s at a vehicle speed of 10km/h.

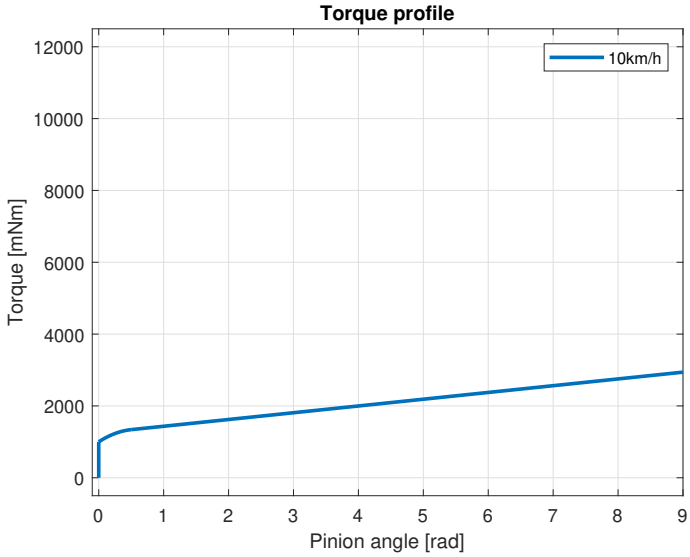

Figure 4.2: *A visualization of the complete base torque profile at 10km/h.*

If the steering wheel would instead be turned such that the movement emulates a sinusoidal wave at a vehicle speed of 10km/h, the base torque curve can be visualized as figure 4.3.

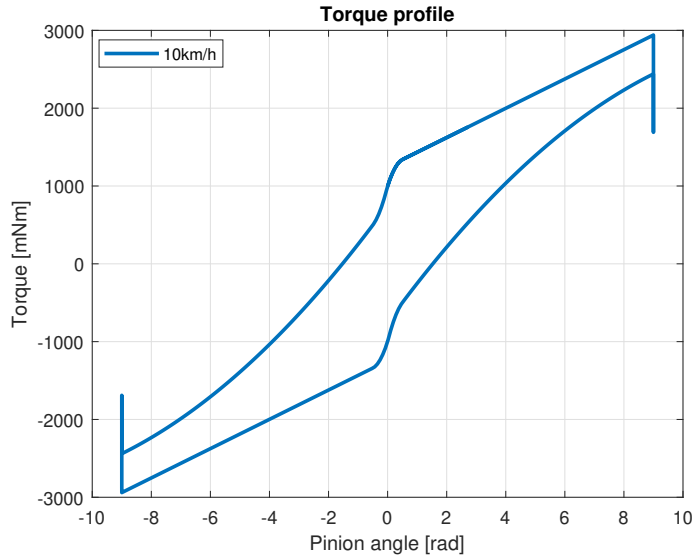

Figure 4.3: *A visualization of the complete base torque profile at 10km/h for a sinusoidal change of steering angle.*

However, there is a problem with the torque profile where it drops at the point of change in turning direction because of how the implementation of the Tanh is done.

4.1.1 Zero velocity torque feature

While stationary, the steering feel of a vehicle is evidently distinguishable compared to a scenario where the vehicle is non-stationary. The largest difference is that if the speed is non-zero an active return will be acting on the steering wheel continually forcing the steering wheel back to the center position. If the velocity is zero, the same forces are not acting upon the steering rack and the steering wheel will not actively return to the center position. Due to the dynamics of the tires, the center position of the active return will move with the change of pinion position. A separate function is therefore created for zero vehicle speed, which was based on a

linear spring-damper model to resemble the forces acting upon the steering rack by the tires to create a torque profile for when stationary.

From EPAS measurements of a stationary vehicle, it was seen that a maximum steering wheel torque of approximately 2000mNm can be achieved if damping is not taken into consideration. It could also be seen that when turning more than approximately 0.5rad the center of the active return is moved the same distance as the new pinion angle subtracted with 0.5rad, see figure 6.17.

Thus was the zero velocity torque profile first designed as a spring with a linearly increasing torque to a maximum value of 2000mNm at 0.5rad and the position of zero torque for the spring is moved with $x - 0.5rad$ where x is a position larger than 0.5rad from the center. On top of this, a linear damping was added. The damping was subjectively tuned in a vehicle for the torque profile to match the EPAS system.

4.2 Loss of traction (Understeer)

When understeer occurs i.e. when the grip between the front tires and the road starts to decrease the steering wheel torque also starts to decrease. It was decided at the beginning of the project that the accuracy of the torque loss from loss of traction was not to be in focus. The torque profile of the loss of traction should be considered more as a part of a trial of concept since the calculations of the angle when the torque loss starts is also heavily simplified.

The torque profile for the loss of traction feature is designed as a second-degree polynomial with a number of tunable parameters for easy adaptability to any previous torque profile and possible succeeding torque profile. The second-degree polynomial was found by setting up an equation system of symbolic variables and solving it to find the equations solving each polynomial parameter. The equation system was defined by the following equations

$$0 = 2a_2 x_{slipStart}^2 + b_2 \tag{4.6a}$$

$$y_{slipEnd} = a_2 x_{slipEnd}^2 + b_2 x_{slipEnd} + c_2 \tag{4.6b}$$

$$y_{slipStart} = a_2 x_{slipStart}^2 + b_2 x_{slipStart} + c_2 \tag{4.6c}$$

where a_2, b_2 and c_2 are the unknown polynomial parameters. The parameter $x_{slipStart}$ is the angle at which the loss of traction torque curve is initiated and the torque should start to decrease, $x_{slipEnd}$ is the angle at which the torque profile should reach its minimum amount of torque, $y_{slipStart}$ is the amount of torque that the torque profile should start with i.e. the amount of torque the was just before the loss of traction torque profile should initiate, and $y_{slipEnd}$ is the minimum amount of torque that can be reached by the loss of traction torque profile. For this project, it was set such that $y_{slipEnd} = 0$ i.e. zero torque will be applied to the steering wheel when all grip has been lost. The parameter $x_{slipStart}$ is continuously calculated from equations 3.9-3.12 and $x_{slipEnd}$ is continuously updated as $1.5x_{slipStart}$. The parameter $y_{slipStart}$ was lastly continuously updated to the same torque value the base torque curve would give at $x_{slipStart}$.

Equation 4.14 defines the condition that the derivative of the torque curve at $x_{slipStart}$ should be 0 such that the torque always directly starts to decrease when the loss of traction feature is initiated. Equation 4.6b defines the condition that the torque should be $y_{slipEnd}$ at $x_{slipEnd}$ which is zero at the angle where all grip has been lost. Equation 4.6c defines the condition that the torque should be $y_{slipStart}$ at $x_{slipStart}$ where $y_{slipStart}$ is the amount of torque just before the loss of traction feature should be initiated such that the starting torque of the torque curve can be ensured to start the same torque as the base torque feature ended.

Solving the equation system gives the following equations for the polynomial parameters

$$a_2 = \frac{y_{slipEnd} - y_{slipStart}}{(x_{slipEnd} - x_{slipStart})^2} \tag{4.7a}$$

$$b_2 = \frac{-(2x_{slipStart}(y_{slipEnd} - y_{slipStart}))}{(x_{slipEnd} - x_{slipStart})^2} \tag{4.7b}$$

$$c_2 = \frac{x_{slipEnd}^2 y_{slipStart} + x_{slipStart}^2 y_{slipEnd} - 2x_{slipEnd} x_{slipStart} y_{slipStart}}{(x_{slipEnd} - x_{slipStart})^2} \tag{4.7c}$$

where equations 4.7a, 4.7b and 4.7c all define the torque profile for the loss of traction feature. See figure 4.4 for examples of the loss torque curve for loss of traction for the two vehicle speeds 30km/h and 60km/h.

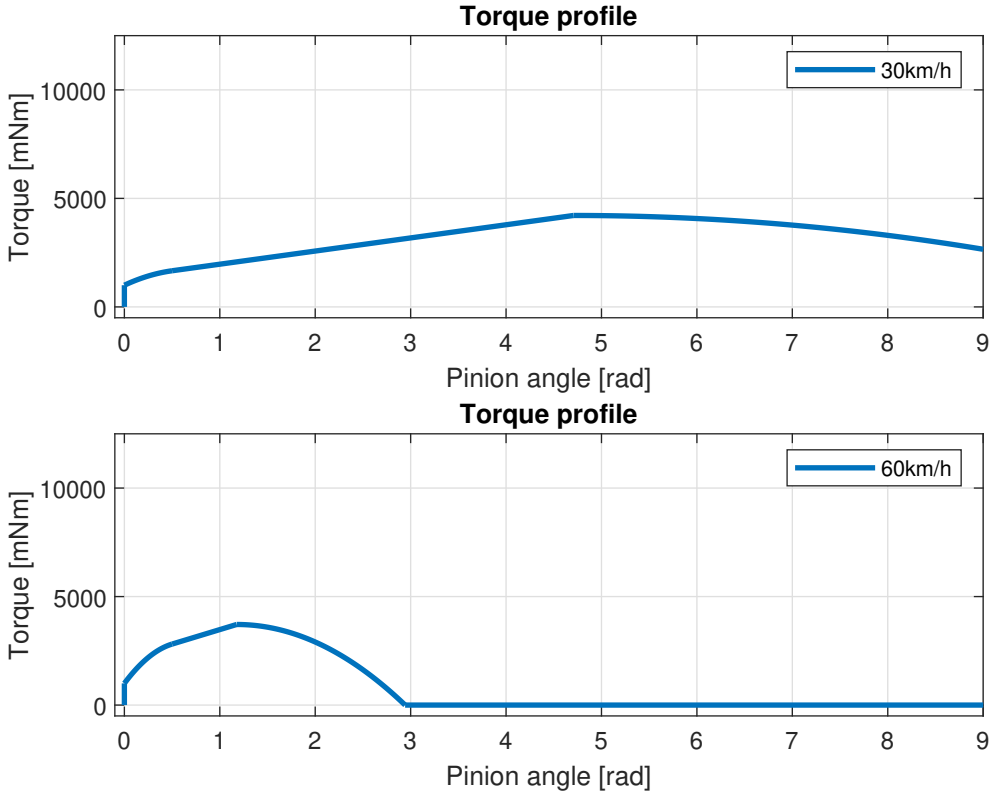

Figure 4.4: *A visualization of the torque loss when grip has been lost for the two vehicle speeds 30km/h and 60km/h.*

4.3 End-stop

All passenger vehicles have steering racks with a maximum travel length i.e. all vehicles have a maximum steering angle. For the general vehicle with an EPAS steering system where the steering wheel is mechanically coupled with the steering rack when the maximum travel length of the steering rack is reached the steering wheel can not be moved further either. Thus for an SbW system, either a mechanical or electrical end-stop has to be additionally implemented. For this particular project with the hardware setup available, an electrical end-stop was chosen to be developed.

To make the torque increase smooth and fast to alert the driver that the maximum steering angle has been reached it was chosen to use a second decree polynomial $y = a_3x^2 + b_3x + c_3$ to generate the torque as a function of the pinion angle which can be seen as non-linear spring. To be able to efficiently tune the end-stop an equation system of symbolic values was set up and solved to find the equations solving the second-degree polynomial parameters. The equation system used to find the polynomial parameters was the following

$$y_{max} = a_3x_{max}^2 + b_3x_{max} + c_3 \tag{4.8a}$$

$$0 = 2a_3x_{end} + b_3 \tag{4.8b}$$

$$y_{end} = a_3x_{end}^2 b_3x_{end} + c_3 \tag{4.8c}$$

where x_{end} is the angle at which the end-stop should initiate i.e. the maximum travel length of the steering rack. The parameter x_{max} is the position at which the end-stop should reach the maximum wanted torque since the FFb actuator can only output a maximum amount of torque. The parameter y_{end} is the amount of torque at which the end-stop should initiate. This parameter is necessary because of the varying base torque profile depending on the vehicle speed since the end-stop should be able to initiate at any current torque. The parameter y_{max} specifies the amount of torque wanted at x_{max} i.e. the maximum amount of torque. The parameters a_3, b_3, and c_3 are the polynomial constants that are of interest to find.

Equation 4.8a specifies that the torque should be y_{max} at x_{max}, equation 4.8b specifies that the slope of the torque at x_{end} should be 0 and equation 4.8c specifies that the torque should be y_{end} and x_{end}.

The solution to the equation system was the following equations for the polynomial constants

$$a_3 = \frac{-(y_{end} - y_{max})}{(x_{end} - x_{max})^2} \tag{4.9a}$$

$$b_3 = \frac{2x_{end}(y_{end} - y_{max})}{(x_{end} - x_{max})^2} \tag{4.9b}$$

$$c_3 = \frac{x_{end}^2 y_{max} + x_{max}^2 y_{end} - 2x_{end}x_{max}y_{end}}{(x_{end} - x_{max})^2} \tag{4.9c}$$

where x_{end}, x_{max}, y_{end}, and y_{max} all are tunable parameters to find the correct end-stop function during vehicle operation.

If the steering wheel would be rotated further than x_{max} a constant torque with the amount of y_{max} will be generated. This torque should be high enough for the driver to acknowledge that the steering wheel should not be rotated further but at the same time not be so high that it requires a large FFb actuator. It was decided that 8000mNm was enough for both conditions to be satisfied. See figure 4.5 below for a visualization of the end-stop torque curve joined with the base torque curves for the vehicle speeds 10km/h, 30km/h, and 60km/h.

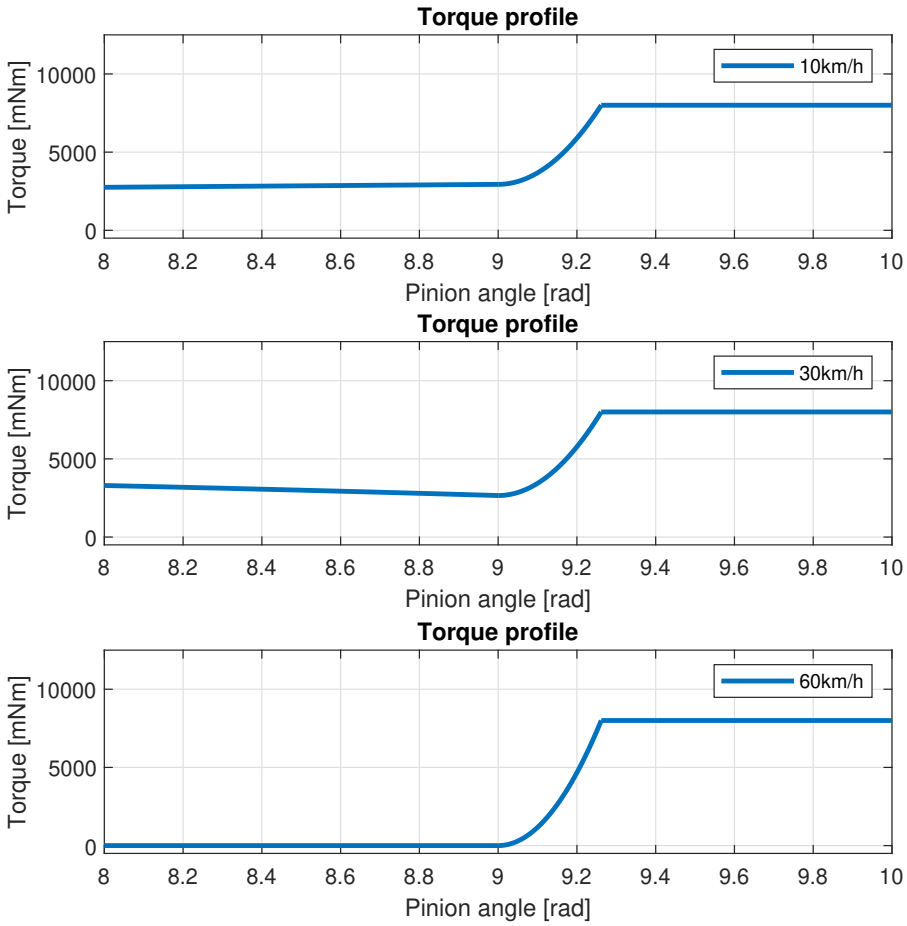

Figure 4.5: *Illustration of the end-stop torque curve initiating at 9rad pinion angle for the vehicle speeds 10km/h, 30km/h, and 60km/h.*

4.3.1 Obstacle detection

Just as the steering wheel should not be further rotated when the steering rack has reached its maximum traveling length for a SbW system without torque feedback, can the steering wheel further be rotated if the wheels happen to be in a locked case e.g. get stuck against a curb or something else inhibiting the wheels to keep turning. The same end-stop torque profile is thus also used for this feature to effectively give feedback to the driver that the wheels can not be further turned called obstacle detection.

For the system to acknowledge that there is an obstacle hindering the wheels from turning the difference between the pinion angle of the steering rack and the steering wheel is constantly checked. If the difference between the angles starts to differ too much the end-stop torque profile is initiated.

4.4 Damping

To achieve pleasant and smooth steering feel similar to that of EPAS while maneuvering a vehicle different types of damping are required. The steering feel model developed and implemented utilizes two kinds of damping, namely On-center and End-stop damping. All types of damping are always added as an additional torque in the opposite direction of the turn of the steering wheel.

4.4.1 On-center damping

The On-center damper was designed for neutralizing steering wheel overshoot achieved at high vehicle speeds when letting the steering wheel return to its zero position when the driver releases the steering wheel. The On-center damper was designed as a Gaussian function with an additional constant term, $y = a_5 e^{-b_5 x^2} + c_5$. The reason behind choosing a Gaussian function is that if the x-axis is dependent on the position of the steering wheel damping will only exist around the origin i.e the center position of the pinion, see figure 4.6 for visualization. The additional constant term added to the Gaussian function is due to the possibility of adding standard linear damping to the system independent of the pinion angle. Since if a constant is added to a curve the curves y-values increase with the same amount for all x-values. Because of unwanted irregular resistance in the system, the constant c_5 was set to zero disregarding any linear damping to the steering feel model.

The amount of damping needed to efficiently neutralize the steering wheel from overshooting needed to be larger for higher vehicle speeds. Thus needed the parameter a_5 is dependent on the vehicle speed because this parameter decides the maximum value of the Gaussian function. A simple equation system was thus set up to find a linear function for a_5 dependent on the vehicle speed as follows

$$\alpha = 80a_6 + b_6 \tag{4.10a}$$

$$\beta = 40a_6 + b_6 \tag{4.10b}$$

where α and β are tuning parameters, α is the amount of damping at the vehicle speed 80km/h, and β is the amount of damping at the vehicle speed 40km/h. The parameters a_6 and b_6 are the function parameters for the linear function. The vehicle speed 40km/h was chosen because it is at a speed higher than that that the steering wheel starts to overshoot. The vehicle speed 80km/h was not chosen for any particular reason, any vehicle speed higher than 40km/h had worked.

By solving the equation system 4.10 the following solution for the linear function parameters was found

$$a_6 = \frac{\alpha}{40} - \frac{\beta}{40} \tag{4.11a}$$

$$b_6 = 2\beta - \alpha \tag{4.11b}$$

where these functions then can be used to define the Gaussian function parameter a_5 as follows

$$a_5 = a_6 \cdot vel_{vehicle\_km} + b_6 = (\frac{\alpha}{40} - \frac{\beta}{40}) \cdot vel_{vehicle\_km} + 2\beta - \alpha \tag{4.12}$$

where $vel_{vehicle\_km}$ is the current vehicle speed in km/h. The complete Gaussian function can now be defined as

$$b_{baseTrq} = a_5 e^{-b_5 x^2} + c_5 \tag{4.13}$$

where $\alpha = 500$, $\beta = 0$, $c_5 = 0$, and $b_5 = 0.2$. The parameter α was tuned from real-life tests where the goal was to find the least amount of damping to neutralize the steering wheel from overshooting. The parameter β was set to zero because at 40km/h zero on-center damping is needed. The active range of the Gaussian function is decided by the value of b_5 and using $b_5 = 0.2$ attains a non-zero value within the interval of approximately [-4:4]rad, see figure 4.6 below. The computed damping constant $b_{baseTrq}$ is then multiplied by the angular velocity of the steering wheel and subtracted from the total reference torque. Additionally, the value of $b_{baseTrq}$ was designed to never attain a value below c_5 to ensure that damping would not change sign if the vehicle speed is less than 40km/h i.e. the on-center damping remained zero for the vehicle speed below 40km/h.

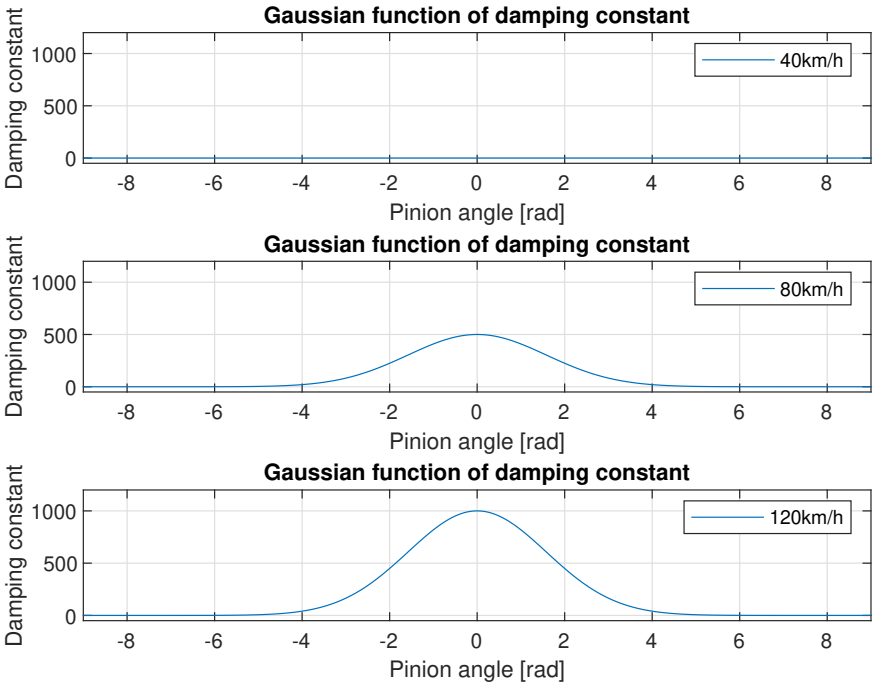

Figure 4.6: *A visualization of three curves for the On-center damping constant for the three vehicle speeds 40km/h, 80km/h, and 120km/h.*

4.4.2 End-stop damping

The End-stop damper was designed to suppress the steering feel of feeling too much as an ideal spring when turning into the End-stop. It was decided that a hyperbolic Tanh function dependent on the pinion angle would be sufficient to define the damping constant. The Tanh function was chosen because the pure Tanh curve starts at zero at the origin and then increases to one when the x-axis goes to infinity. This can be utilized such that the damping constant for the End-stop is initialized as zero at the moment the End-stop is initiated and then smoothly increases to a desired maximum value with a desired speed. The End-stop damping feature was constructed as follows

$$b_{endStop} = \frac{e^{4x} - 1}{e^{4x} + 1} \cdot b_{end} \tag{4.14}$$

where the constant $b_{end} = 700$ determines the maximum value of the damping constant, $x = pos - x_{end}$ where pos is the current position of the steering wheel and x_{end} is, as mentioned in section 4.3 when the End-stop torque profile is initiated and the number four in the exponent determines the gradient of Tanh at the origin and causes the function to almost fully converge at 1rad. Compared to previous use cases of the Tanh function, x is the difference between the current pinion angle and the initial end-stop position. The damping constant is multiplied by $vehicle_{vel}^2$ to get the amount of torque for the damping, which gives non-linear damping to the system for the End-stop feature.

4.5 Displacement of zero torque position (Oversteer)

In the early stages of the project, it was decided that a feature that simply allows the possibility of simulating what happens with the torque at an oversteer scenario. Oversteer occurs when a vehicle is affected by a loss of traction of the back wheels and the actual turning trajectory is greater than the reference trajectory, see figure 4.7 for a visualization. When this happens the position where the steering wheel has zero torque is moved such that the new zero torque position is centered with the actual trajectory of the vehicle. The position where the torque is zero will always be in the center of the trajectory of the vehicle. Adding a variable that can be used to add a displacement of the zero torque position of the steering wheel, makes it possible to simulate what happens with the torque profile when oversteering.

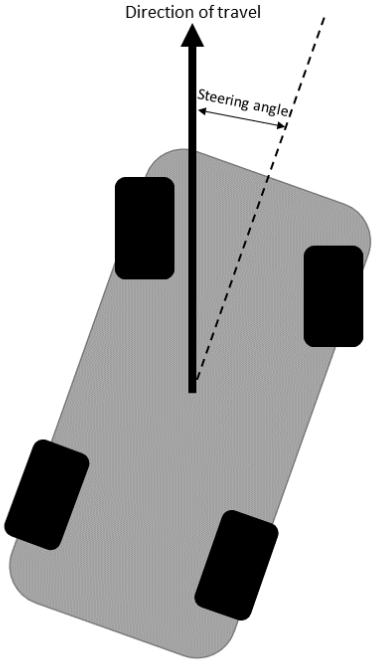

Figure 4.7: *An illustration of an oversteer scenario.*

A variable was added for inserting a displacement of the zero torque position as a track bar that could be adjusted during real-time testing and evaluation. When a displacement is added, the base torque profile and damping are adjusted to the current zero torque position but the end-stop and loss of traction during understeer positions remain fixed. No additional algorithms were developed or implemented for how the displacement of the zero torque position should alter the base torque profile or the understeer profile. The variable for the displacement of the zero torque position was named $pos_{shifted}$ and was calculated as

$$pos_{shifted} = pos - shift \tag{4.15}$$

where pos is the current pinion angle and $shift$ is the shift made by the displacement.

4.6 Return to center

Due to mechanical friction and the cogging torque affecting the system, the steering wheel does not always return to its center position with base torque alone. Therefore, two methods for compensating these forces have been implemented. In reality, the steering wheel does not return to the center position for all vehicle speeds but for this project, it is assumed that the steering wheel always should return to its center position regardless of the vehicle speed. Unless the vehicle is stationary.

The first method is called friction compensation where the sum of the mechanical friction and the cogging torque is assumed to be constant for simplicity. The friction compensation is designed such that the value of y_2

for the base torque is adjusted by adding a constant torque $T_{fricComp}$ in the turning direction. If the steering wheel is rotated away from the center position y_2 is subtracted with a constant torque and if the steering wheel is rotated to the center position a constant torque is added to y_2. By doing so, the slope and amount of torque for the entire torque profile are adjusted to the new value of y_2 at x_2 i.e. the complete base torque profile has been adjusted from the friction compensation accordingly with the rotation direction of the steering wheel.

For the steering wheel to always return to the center position, independent of the vehicle speed, the constant $T_{fricComp}$ was set to a value of 1000mNm to overcome both the mechanical friction and the cogging torque. The constant value was found from real-time testing of the system in the testing rig.

The second method is to add an integrating part $T_{integrator} = \sum K_i error$ to the steering feel model with the zero torque position as the reference value of the error. Due to the hysteresis of the overall torque profile, a fast-acting integral part is required for small angles to compensate for when the mechanical friction and cogging torque are greater than the base torque. For angles within the interval of $abs(steering\ wheel\ angle) < 1rad$ the error equals

$$error = \frac{1}{x} \tag{4.16}$$

where x is the pinion angle. For $abs(steering\ wheel\ angle) \geq 1rad$ the error equals

$$error = x. \tag{4.17}$$

The integral part is updated with a frequency of 100Hz with a maximum step value for each iteration. An integral gain of $K_i = 1.5$, a maximum step size of 10mNm, and a maximal value of the integral generated torque equal to $T_{integrator_max} = 750$mNm were chosen to achieve satisfactory results where the steering wheel returns to its center position for all vehicle speeds.

4.7 Angular velocity limiter

Because the steering rack actuator has a maximum angular speed of 6rad/s the steering wheel and the steering rack might end up unsynchronized if the steering wheel is rotated faster than 6rad/s. This would mean that the difference between the steering rack actuator pinion angle and the pinion angle would be nonzero which would mean that the obstacle detection could be initiated, see section 4.3.1. This would give feedback to the driver that the wheels are stuck to something rather than the steering wheel has been rotated too fast.

To prevent this from happening an Angular velocity limiter could be used to impede the driver from actually being able to turn the steering wheel faster than 6rad/s. Two different velocity limiters were briefly developed and tested because of it not being a priority and not enough time was available to fully develop and evaluate this feature.

The first velocity limiter was developed as a PI controller where the goal was to generate an additional torque as feedback to prevent the driver from rotating the steering wheel too fast. The control scheme was constructed such that the PI-controller only was active if the pinion angular velocity was over 5.5 rad/s. The number 5.5 was chosen to give the controller some margin in case the controller was too slow to directly apply the correct amount of torque as soon as the steering gets unsynchronized without overshoot and instability. The control algorithm was based on the acceleration of the steering wheel in such a way that the control algorithm uses the acceleration as its reference signal with a setpoint of zero to generate a control signal i.e. a torque in the opposite direction of the acceleration with the goal to keep the acceleration of the pinion at zero.

The second velocity limiter was developed as a nonlinear damper to hinder the driver from turning the steering wheel too fast. The disadvantage with the damping instead of the PI-controller is that the pinion velocity can not be controlled using acceleration with the goal to make it impossible for the driver to rotate the steering wheel too fast. The damper instead generates a torque depending on the pinion velocity which does not depend on the torque the driver turns the steering wheel with. This means that the driver could turn with a higher torque than the angular velocity limiter generates and the speed of the steering wheel could then in theory be faster than the maximum allowed speed. But just as the End-stop feature the goal is just to give the driver enough information that something is wrong, and in this particular case informing the driver that the steering wheel is being rotated too fast.

The nonlinear damper was designed as $T = bx^2$ where T is the damping torque, b is the damping constant, and x is the angular velocity of the pinion. A damping constant of 5000 was found to give the desired amount of damping. Due to the fact that the damping is a feature to prevent the driver from turning the steering wheel

too fast and not affect the overall steering feel by adding unnecessary damping, the damping only affects the steering feel if the steering wheel is rotated faster than 4rad/s. Due to the limitations of the FFb actuator, a maximum amount of damping torque was set to 20000mNm if the steering wheel is to be rotated faster than 6rad/s.

5 Vehicle handling tests

There are multiple tests for evaluating the steering feel of a vehicle. For the passenger vehicle industry, a number of internationally standardized tests have been developed to evaluate the steering feel of any passenger vehicle. For this project, one standardized test and two unstandardized tests have been used. The following tests were utilized for evaluating the relation between pinion torque and position for SbW systems.

The Weave test is a standardized test developed to evaluate the handling characteristics of a passenger vehicle during maneuvers performed at higher vehicle speeds [10]. A low-frequency sinusoidal steering maneuvering is performed during the test that allows for measurements accurately describing the relation between the steering wheel angle and steering wheel torque but in this case the pinion angle and steering wheel torque. The output data provides a steering hysteresis describing the on and off-center torque slope behavior difference between turning away from the center position at a certain degree and back. See figure 5.1 below for an example of the motion of the pinion during a weave test.

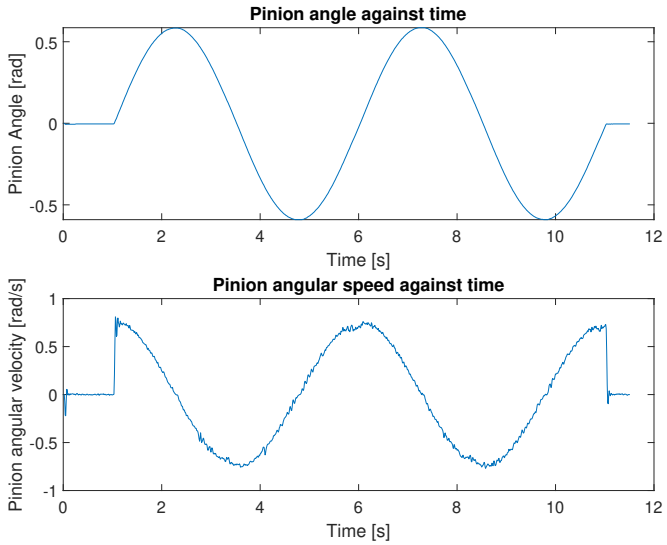

Figure 5.1: *Image illustrating pinion angle and pinion angular velocity for a Weave test*

The Ramp steer test is a test that was used to evaluate the handling characteristics while conducting steering maneuvers consisting of linearly increasing the steering wheel angle position at a slow and fixed angular velocity. The test is performed within a fixed position interval from the center position to a predetermined final value. This allows for accurate measurements describing the relation between pinion torque and position at slow pinion velocities at different vehicle speeds. See figure 5.2 below for an example of the motion of the pinion during a Ramp steer test.

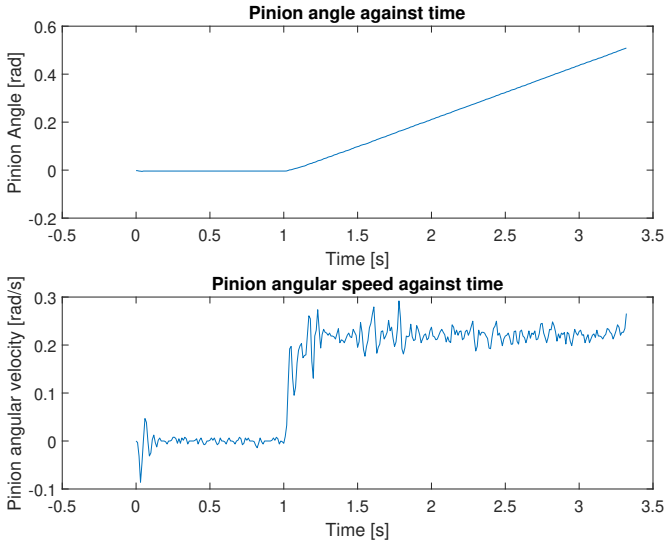

Figure 5.2: *Image illustrating pinion angle and pinion angular velocity for a Ramp steer test*

Return to Center test is a test that was used to evaluate and demonstrated the ability of the steering wheel to return to the center if let go. The test was conducted by turning the steering wheel to the maximum torque peak at a certain vehicle speed before arriving at the end-stop and then releasing the steering wheel such that the steering wheel could return to its center position without any external forces acting upon it.

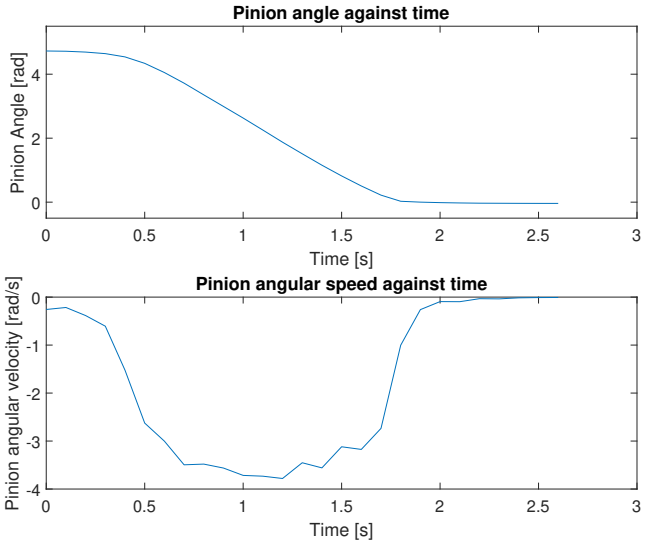

Figure 5.3: *Image illustrating pinion angle and pinion angular velocity for a Return to Center test*

6 Experimental results

The results of performing a set of different handling tests on the steering feel model, combined with different assisting features for returning to the center, are shown in this chapter in comparison with the EPAS measurements used to develop the steering feel model. All combinations of features for the steering feel model include the Base torque, the End-stop feature, and the Loss of traction feature. The set of tests performed was Ramp steer, Weave, and Return-to-center which have been described in chapter 5. The tests were performed on different variants of the steering feel model. The chapter is divided into the following sections.

- Base torque: Illustrates the results of performed Ramp steer tests, Weave tests, and Return to center tests of solely the base torque, the understeer feature, and the end-stop. The results are then compared to those of an EPAS system to show the resemblance of the torque generation between the SbW system and an EPAS system.
- Base torque with On-center damping: Illustrates the results of performed Ramp steer tests, Weave tests, and Return to center tests of the base torque with On-center damping, the understeer feature, and the end-stop. The results are then compared to those of an EPAS system to show the resemblance of the torque generation between the SbW system and an EPAS system.
- Base torque with additional Return to zero features: Illustrates the results of performed Ramp steer tests, Weave tests, and Return to center tests of the base torque with additional return to center assistance, the understeer feature, and the end-stop. The results are then compared to those of an EPAS system to show the resemblance of the torque generation between the SbW system and an EPAS system.
- Torque at zero velocity: Illustrates the results of the torque generation for a stationary vehicle as a comparison between the SbW system and an EPAS system.
- Displacement of zero torque position: Illustrates the results of performed Ramp steer tests for both steering directions, Weave tests, and return to center tests for both steering directions. The torque is generated as solely the base torque, the understeer feature, and the end-stop combined with an additional displacement of the zero torque position.
- Test track: Illustrates the results of performing a driving test conducted on a short and long test track by displaying the measured torque curve of the steering wheel and the measured pinion angle for the SbW system. The results are then compared to the corresponding measurements performed by an EPAS system on the same test tracks.
- Cogging torque: Illustrates the results of the cogging torque affecting the system by performing a test showing the torque curve of the steering wheel from standstill to moving while continuously increasing the motor torque. The tests illustrate the difference between the FFb actuator utilizing and not utilizing cogging compensation.

For all figures of the Ramp steer test follow that the dotted lines represent data taken from measurement on an EPAS system, the solid lines represent the reference torque generated by the steering feel model, and the dashed lines represent the torque estimated by the FFb actuator currently applied to the steering wheel. For all figures of the Weave test, the yellow lines represent the EPAS measurements, the orange lines represent the FFb actuator estimated torque and the blue lines represent the reference torque. All tests except the EPAS measurements were performed by human hands, hence human error might concur.

6.1 Base torque

The following figure 6.1 illustrates a Ramp steer test performed on the steering feel model for the base torque without any return to center assisting features. For all vehicle speeds, namely 3.6km/h, 30km/h, 45km/h, 60km/h, 80km/h, and 100km/h, the reference torque profile resembles the profile generated from the EPAS measurements accurately with low deviation for the data that was available. The differences in the torque profile while increasing the vehicle speed are the initial slope gradients before the pinion angle $x_2 = 0.5$ hence increasing the value of y_2, as well as a quadratic increase of the slope gradient of the linear function beyond the pinion angle $x_2 = 0.5$. Additionally, the pinion angle at which loss of traction occurs for an understeer scenario

is quadratically decreasing. For 3.6km/h, there are no EPAS measurements and the torque profile is linearly increasing beyond $x_2 = 0.5$ until the End-stop.

The irregularities of the estimated torque are the result caused by the cogging torque with fluctuating values between a range of [-400:400]mNm from the reference torque. However, its mean still follows the reference torque accurately.

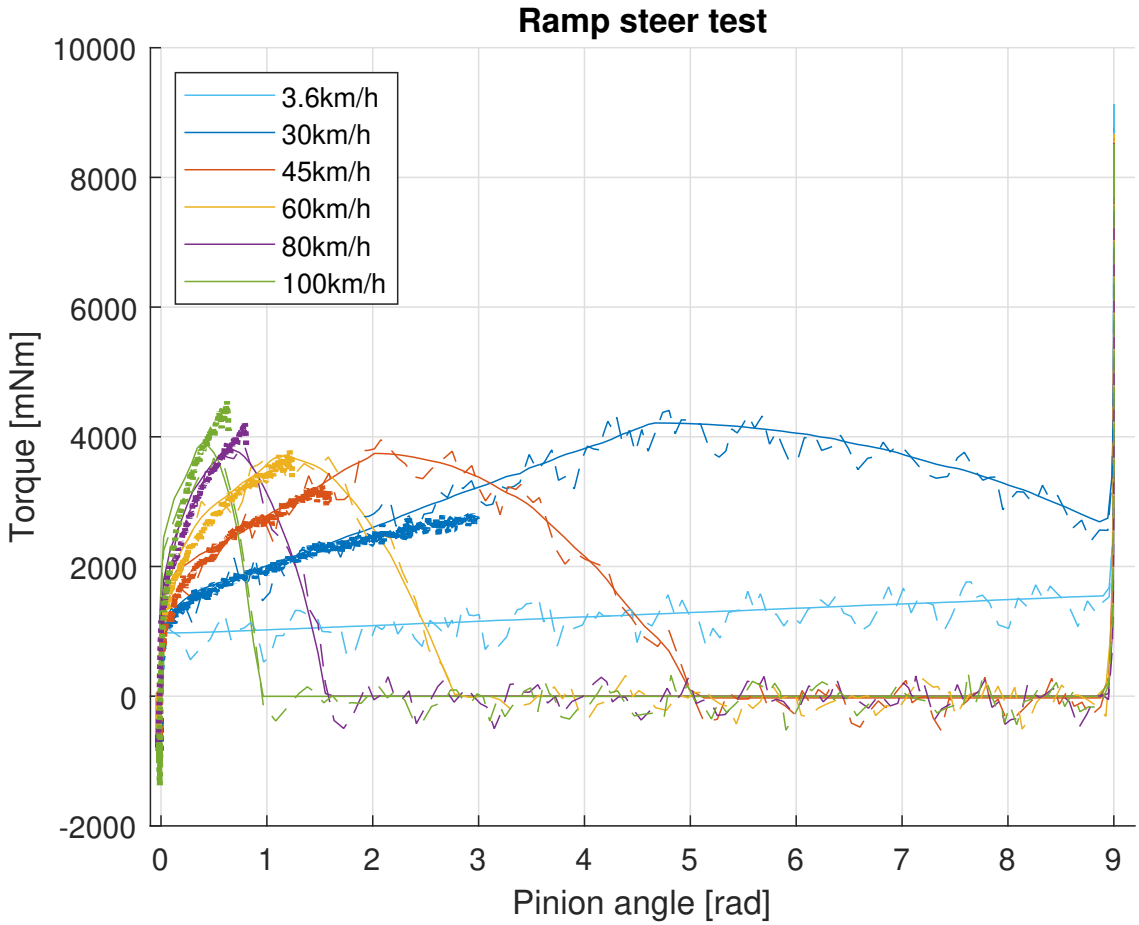

Figure 6.1: *Resulting base torque as a function of pinion angle after performed Ramp steer test. The solid lines are the reference torque generated by the reference generator, the dashed lines are the estimated torque acting on the steering wheel, and the dotted lines are the torque taken from measurement in an EPAS vehicle.*

The Weave test results are illustrated in figure 6.2 for a scenario with the same steering feel model, performed on the same set of vehicle speeds. The reference torque closely follows the EPAS measurements for low vehicle speeds when turning away from the center position, but the distance between the initial slope gradients in the x-axis decreases as the vehicle speed increases. Hence, for higher vehicle speeds, the reference torque profile differs from the EPAS measurements for small pinion angles. In the instance when changing the steering direction toward the center position, the difference in the resulting torque from the SbW system and the EPAS measurements is noticeable but adjusts immediately. The zero torque position of the steering rack with a specific angular velocity profile deviates from the measurements resulting in an incremented position when zero torque occurs. This is the result of the torque profile having a steeper slope gradient with in general a lower mean torque value while turning towards the center position. This behavior holds true for all vehicle speeds. No definitive effects of the cogging torque can be seen for the Weave test because of the very limited range of motion of the steering wheel.

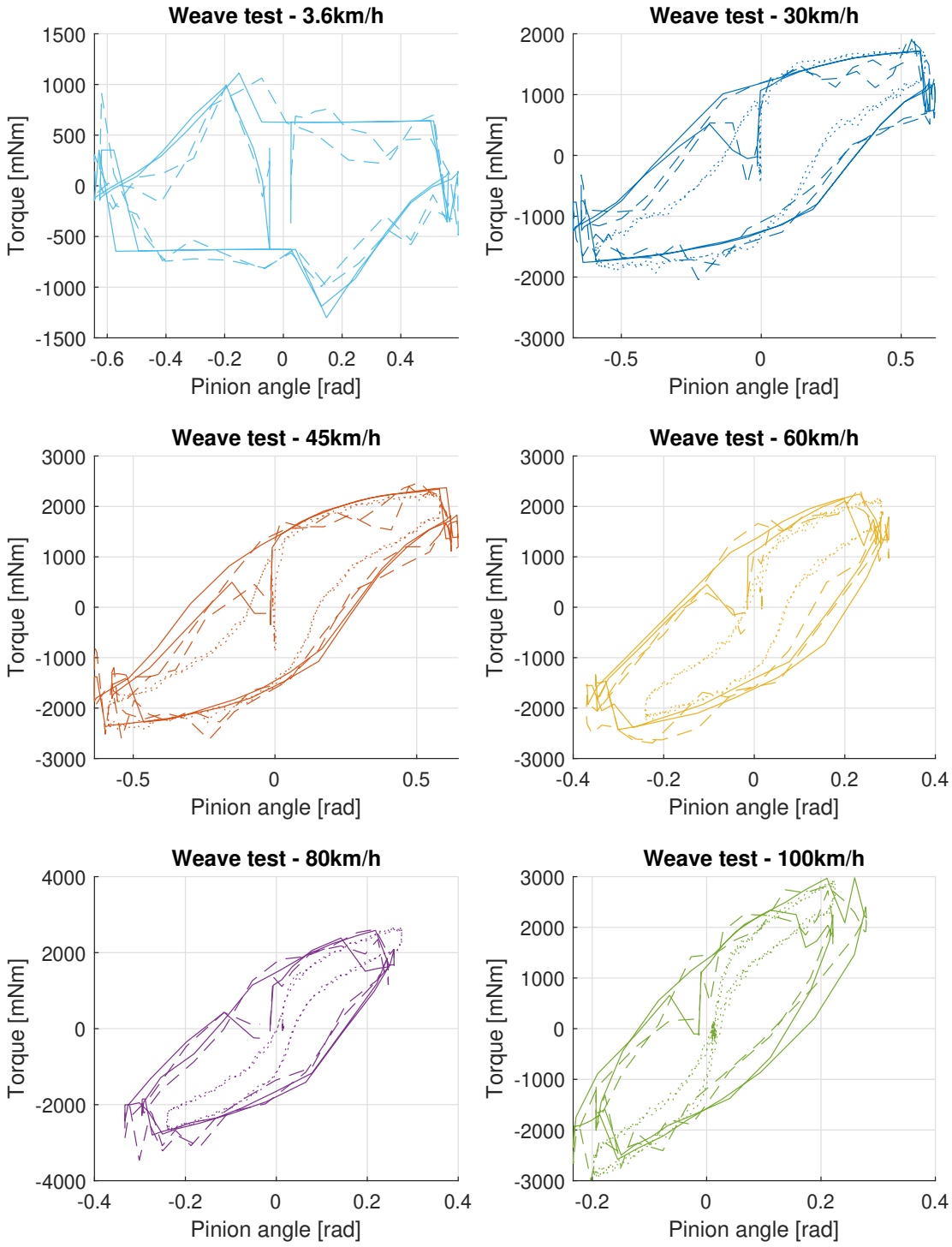

Figure 6.2: *Resulting base torque as a function of pinion angle after performed Weave test. The solid lines are the reference torque generated by the reference generator, the dashed lines are the estimated torque acting on the steering wheel, and the dotted lines are the torque taken from measurement in an EPAS vehicle.*

By performing a Return to center test on the steering feel model with no additional assisting features, the following results were found and are illustrated in figure 6.3.

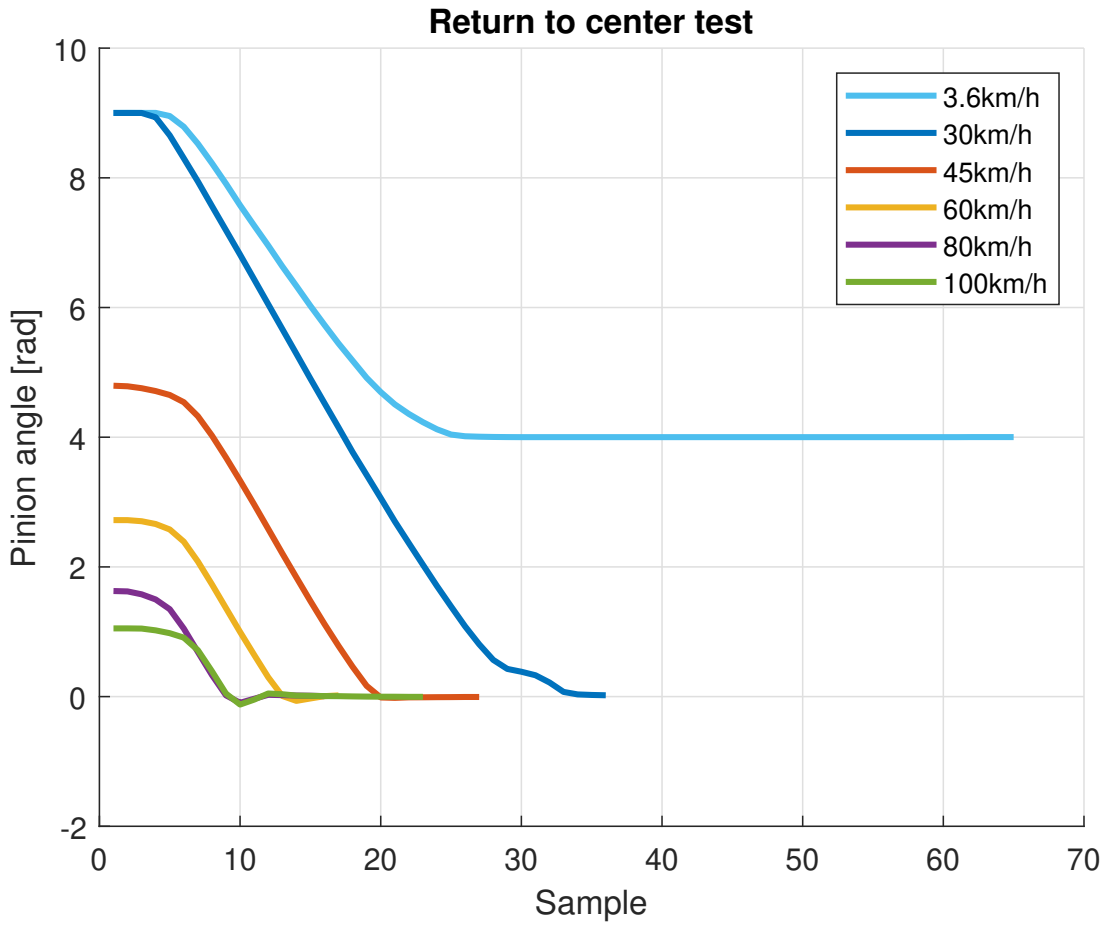

Figure 6.3: *An illustration of how the pinion angle changes during a Return to center test with solely base torque.*

The test was performed at five different vehicle speeds, 3.6km/h, 30km/h, 45km/h, 60km/h, 80km/h, and 100km/h. Figure 6.3 shows that the steering wheel returns to the center position for all vehicle speeds except 3.6km/h. When performing the test at 30km/h the steering wheel does return to center with a discontinuity due to getting stuck at a cogging torque peak. For all remaining vehicle speeds larger than 30km/h, the steering wheel returns to the center position without any discontinuities but is instead affected by an overshoot which grows larger for higher vehicle speeds.

6.2 Base torque with On-center damping

To measure the impact of adding on center damping to the steering feel model, a Ramp steer test was performed at six different vehicle speeds, namely 3.6 km/h, 30 km/h, 45 km/h, 60 km/h, 80 km/h, and 100 km/h. The resulting torque profiles can be observed in figure 6.4. The reference torque profiles closely follow the EPAS measurements with no large deviation. There are no EPAS measurements for 3.6 km/h. For 30 km/h, the reference torque profile has a brief increase in torque for pinion angles beyond 2rad. The torque profile for different vehicle speeds does not follow a consistent behavior of reaching zero torque following the same second-degree loss of traction slope. Instead, for angles approaching zero torque, the profile shows non-linear behavior resulting in a slowly decreasing torque profile until reaching zero. This behavior is true if the pinion angle is below 5 rad. The estimated FFb torque profile is affected by the cogging torque resulting in fluctuations in the torque profile as can be seen by how the dashed lines fluctuate around the solid lines, illustrated in figure

6.4.

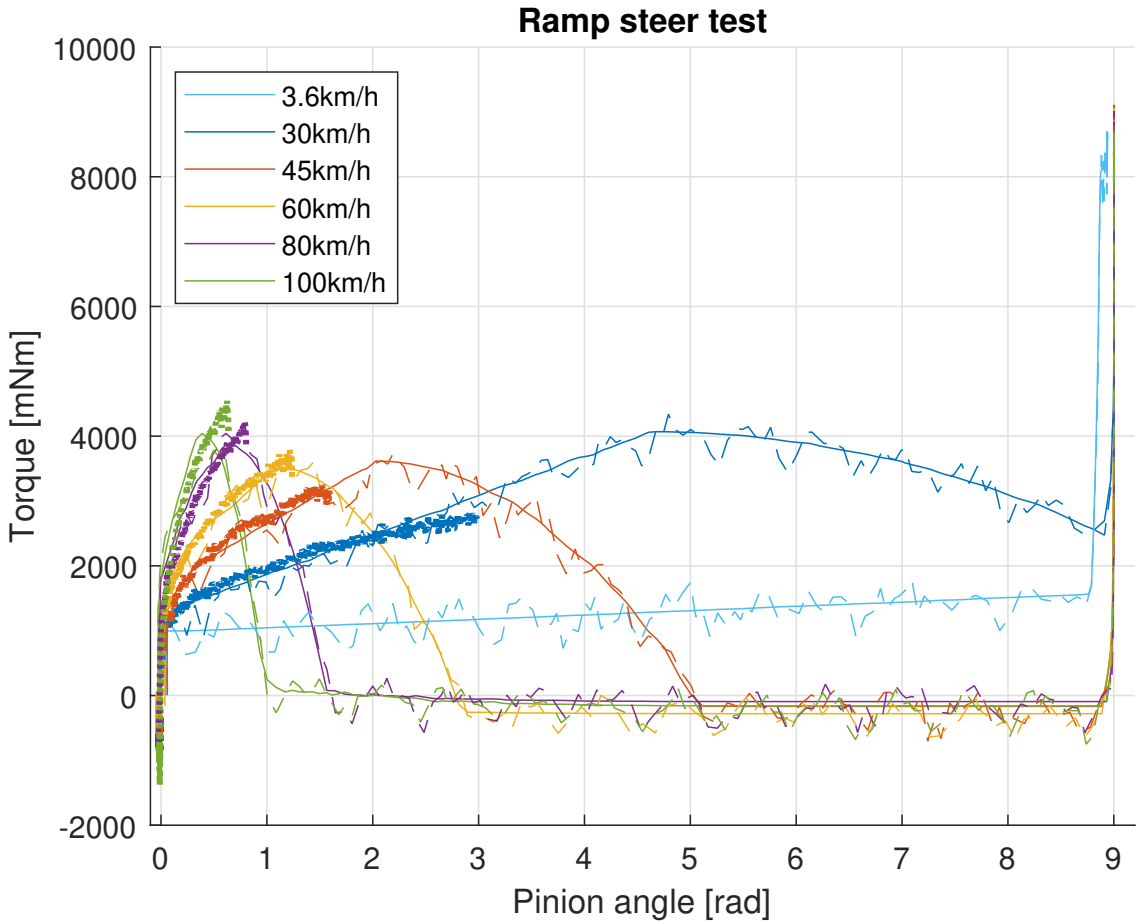

Figure 6.4: *Resulting base torque combined with on-center damping as a function of pinion angle after performed Ramp steer test. The solid lines are the reference torque generated by the reference generator, the dashed lines are the estimated torque acting on the steering wheel, and the dotted lines are the torque taken from measurement in an EPAS vehicle.*

Figure 6.5 illustrates the results after the Weave test for the vehicle speeds 3.6 km/h, 30 km/h, 45 km/h, 60 km/h, 80 km/h, and 100 km/h. The Weave test is performed with base torque combined with the On-center damping feature active. By observing the different torque profiles, the reference torque profile closely follows the EPAS measurements when turning away from the center position. However, for vehicle speeds above 45 km/h, the initial torque gradients of the reference torque profile increase faster than that of the EPAS measurements. Resulting in a steeper slope with higher torque for all small pinion angles. When changing steering direction towards the center position, the reference torque profile generally for all vehicle speeds tends to reach zero torque for a larger pinion angle, with a bigger difference for an increase in vehicle speed. Hence, the characteristics of the hysteresis have changed with a peak torque difference between turning away and turning towards the center position. The torque also drops in value during the instance of changing steering direction but quickly adjusts to the EPAS measurements. Compared to figure 6.2 where no On-center damping is active, the Weave tests show great similarity with minor discrepancies.

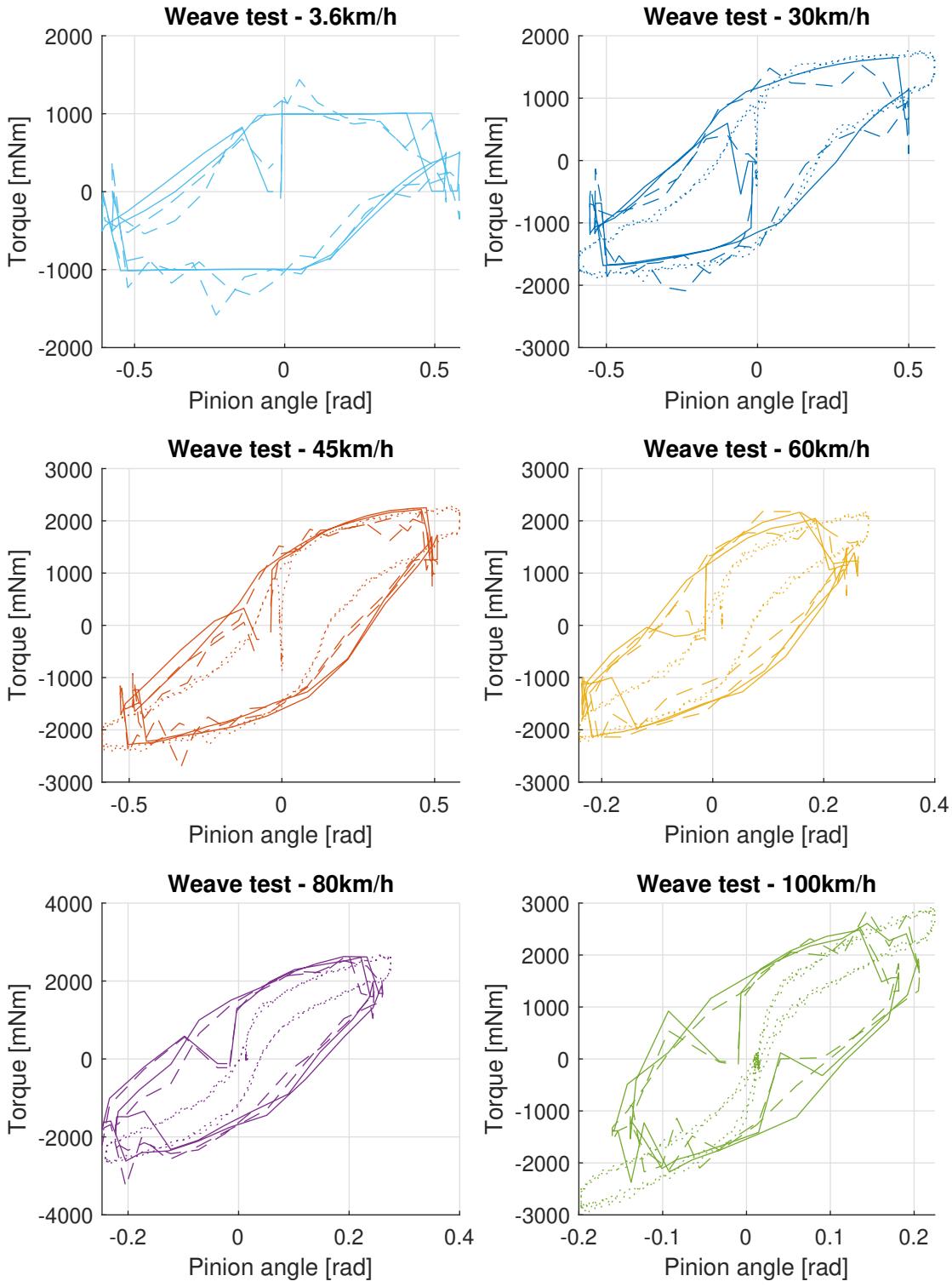

Figure 6.5: *Resulting base torque combined with on-center damping as a function of pinion angle after performed Weave test. The solid lines are the reference torque generated by the reference generator, the dashed lines are the estimated torque acting on the steering wheel, and the dotted lines are the torque taken from measurement in an EPAS vehicle.*

To measure the effectiveness of adding on center damping to the steering feel model, a return to center test was performed for six different vehicle speeds, namely 3.6 km/h, 30 km/h, 45 km/h, 60 km/h, 80 km/h, and 100 km/h which is illustrated in figure 6.6. For all vehicle speeds except 3.6 km/h, the steering wheel returns to the center position. For 30 km/h, the steering wheel stops for a short period of time before reaching the center position. The test results for the remaining vehicle speeds resulted in a smooth transition to the center position with next to no overshoot.

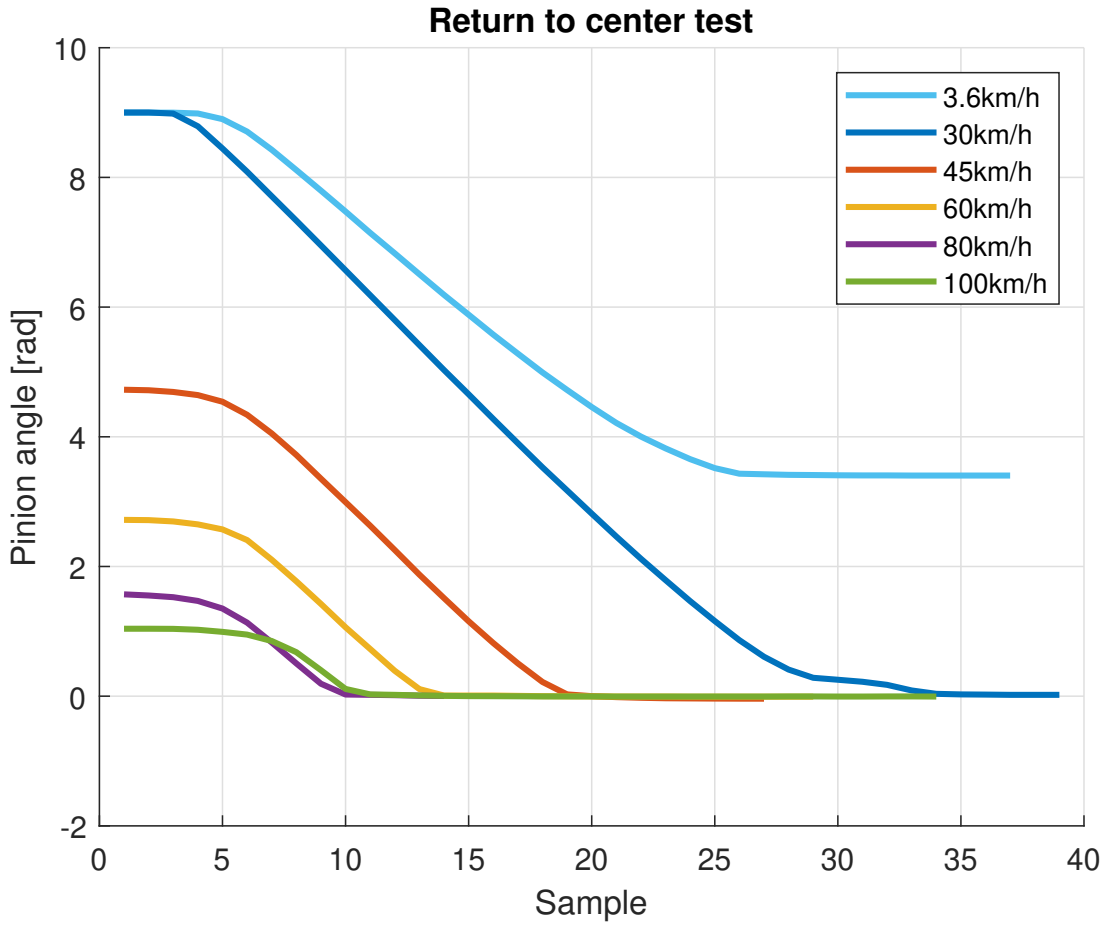

Figure 6.6: *An illustration of how the pinion angle changes during a Return to center test with base torque combined with on-center damping active.*

6.3 Base torque with additional Return to zero features

This section shows the results of the steering feel model with the additional Return to center features Friction compensation and integration.

6.3.1 Return to center assistance by friction compensation

By performing a Ramp steer test on the steering feel model with an additional friction compensation the following results were found, see figures 6.7 and 6.8. Figure 6.7 shows the results of the Ramp steer test on the steering feel model with friction compensation in comparison to the EPAS measurements for the vehicle speeds 30km/h, 45km/h, and 60km/h. Figure 6.8 shows the Ramp steer test on the steering feel model with friction compensation in comparison with the steering feel model without return to center assistance for the vehicle speed 3.6km/h.

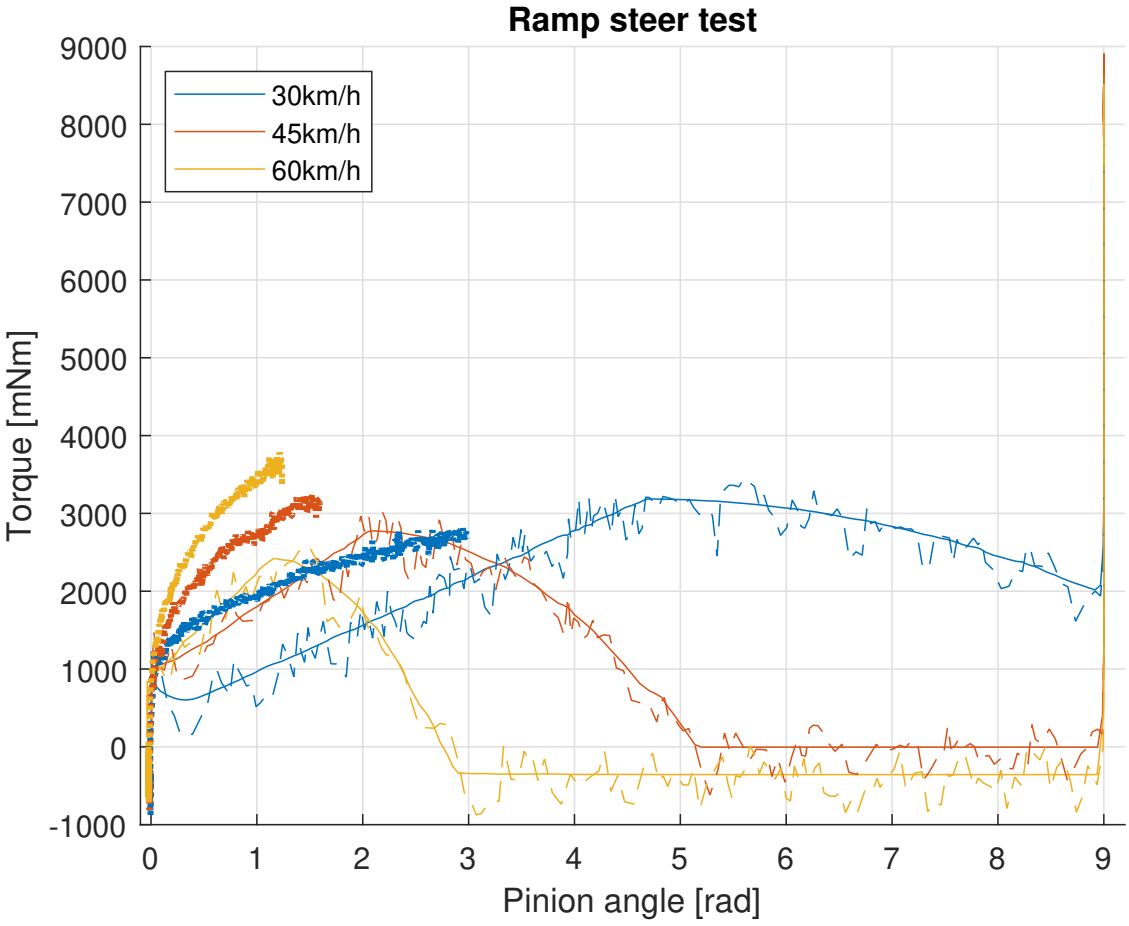

Figure 6.7: *Resulting base torque combined with a return to center assisting friction compensation as a function of pinion angle after performed Ramp steer test. The solid lines are the reference torque generated by the reference generator, the dashed lines are the estimated torque acting on the steering wheel, and the dotted lines are the torque taken from measurement in an EPAS vehicle.*

Figure 6.7 shows the torque measurements taken from an EPAS system on which the base torque is based, the reference torque generated by the reference generator, and the estimated torque acting on the steering wheel. It can be clearly seen that the reference torque and the estimated torque for all vehicle speeds rapidly increase to approximately 1000mNm but then dips such that the torque has an approximate 1000mNm offset from the EPAS measurements for all pinion angles larger than 0.5. The results show that due to the friction compensation necessary to assure the steering wheel returns to center the overall steering feel is negatively

affected since the reference torque nor the estimated torque follows the EPAS measurements for none of the vehicle speeds. In addition, the friction compensation also gives the undesired characteristic at the beginning of the turn at 30km/h, where the torque quickly increases to 1000mNm but then decreases before it starts to increase with the pinion angle at the same rate as the EPAS measurements. If figure 6.7 is compared with figure 6.1 it can clearly be seen that the resulting torque profile is worse with friction compensation if compared to the EPAS measurements.

Figure 6.8 below shows the reference torque and the estimated torque at 3.6km/h where no EPAS torque measurements were available.

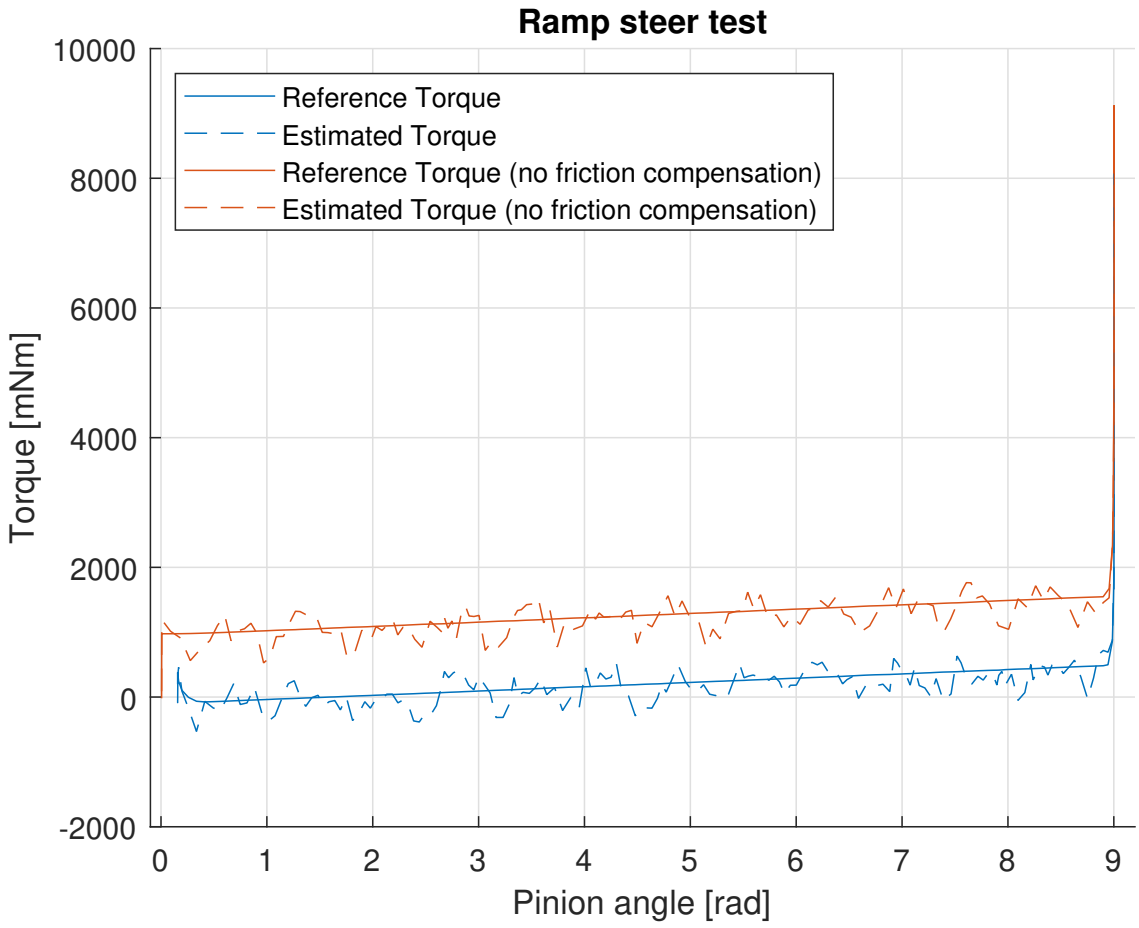

Figure 6.8: *Resulting base torque combined with a return to center assisting friction compensation as a function of pinion angle after performed Ramp steer test. The solid lines are the reference torque generated by the reference generator, and the dashed lines are the estimated torque acting on the steering wheel.*

Figure 6.8 shows how the torque very slightly increases with the pinion angle when friction compensation is applied in comparison to no friction compensation. It can also be seen how the torque slightly increases at the beginning of the turn but then decreases and even becomes negative before it starts to increase with the pinion angle.

Figure 6.9 and 6.10 instead shows the torque profile of the steering feel model with additional friction compensation after a Weave test where figure 6.9 is for vehicle speeds of 30km/h, 45km/h and 60km/h and figure 6.10 is for 3.6km/h.

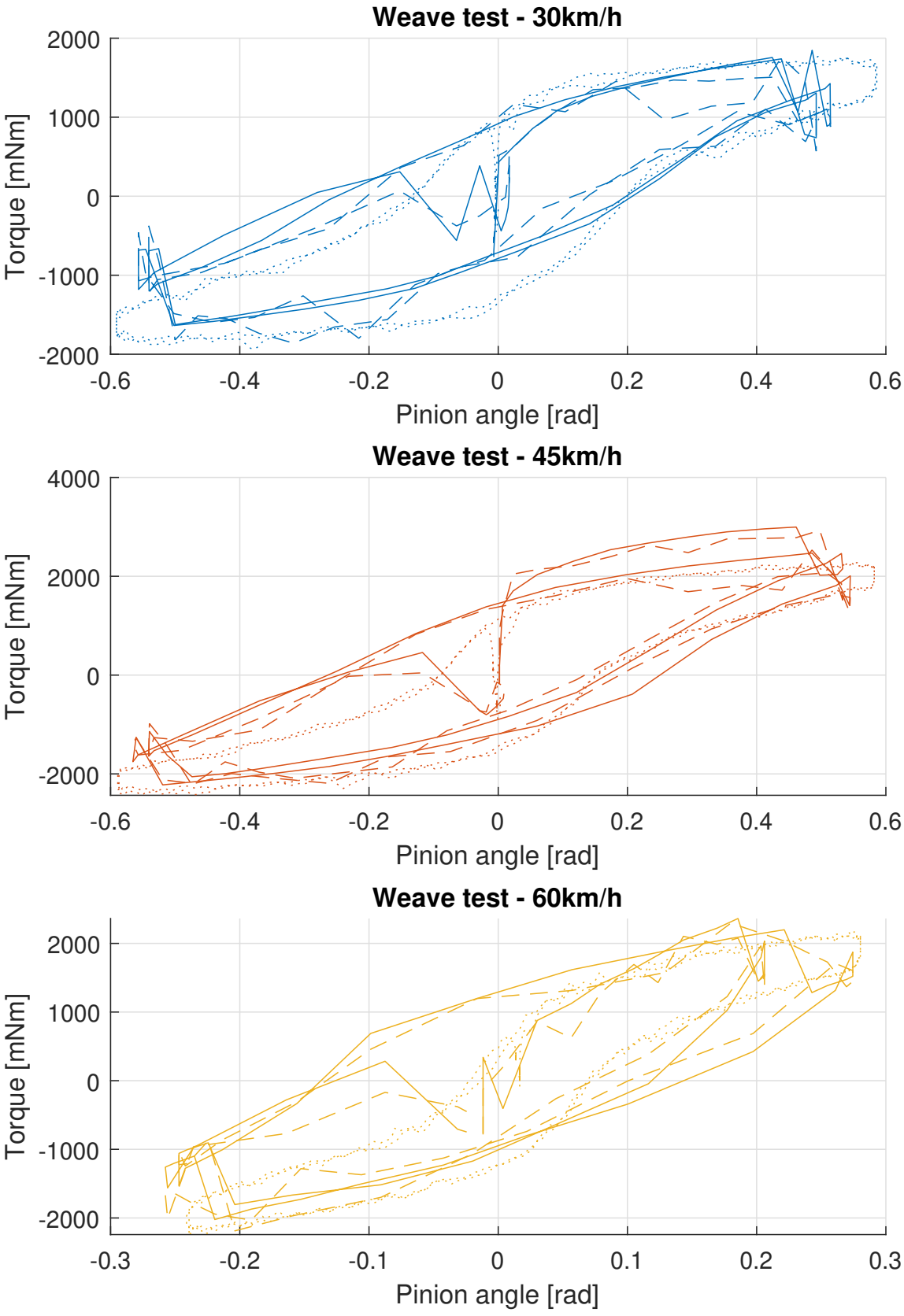

Figure 6.9: *Resulting base torque combined with a return to center assisting friction compensation as a function of pinion angle after performed Weave test. The solid lines are the reference torque generated by the reference generator, the dashed lines are the estimated torque acting on the steering wheel, and the dotted lines are the torque taken from measurement in an EPAS vehicle.*

Figure 6.9 shows how the reference torque and estimated torque differ from the EPAS measurements. As it can be seen from figure 6.9, the reference and the estimated torque do not follow the EPAS measurements. The resemblance to the EPAS torque curve is heavily decreased for all vehicle speeds. As was seen from the Ramp steer tests, the torque first increases but then decreases when driving at 30km/h. When the steering wheel is turned the other way the torque instead increases by approximately 1500mNm instead of decreasing by 500mNm which gives a completely different characteristic to the hysteresis. If figure 6.9 is compared with figure 6.2 it can be clearly seen that the torque profile is completely different and does not resemble the EPAS measurements as intended.

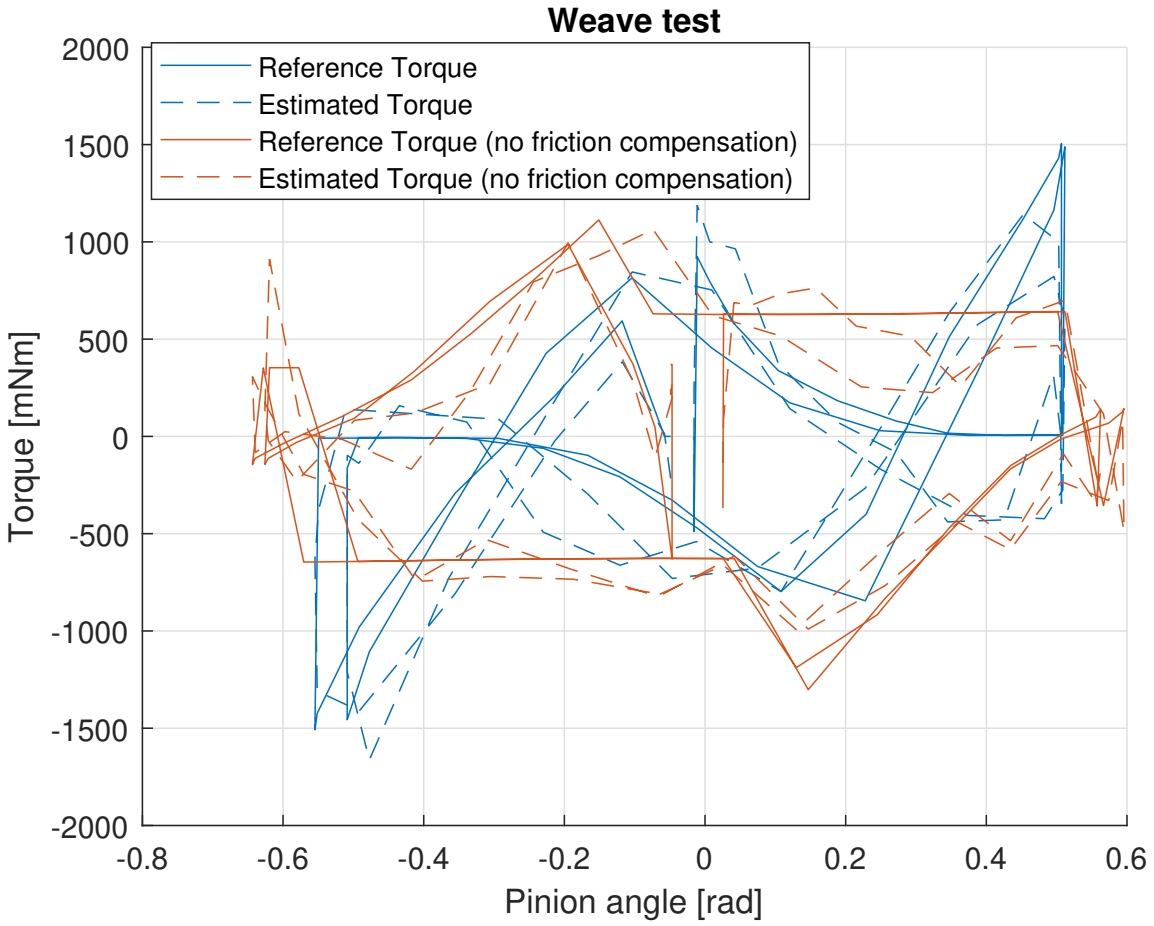

Figure 6.10: *Resulting base torque combined with a return to center assisting friction compensation as a function of pinion angle after performed Weave test. The solid lines are the reference torque generated by the reference generator, and the dashed lines are the estimated torque acting on the steering wheel.*

Figure 6.10 shows the reference torque and estimated torque in comparison to the case with no friction compensation where it can be clearly seen that the characteristics of the EPAS torque curve have been completely lost.

Figure 6.11 shows how well the steering wheel returns to its center at 3.6 km/h, 30km/h, 45km/h, and 60km/h from a performed Return to center test. As it can be seen the steering wheel does return to the center very linearly for all vehicle speeds. Until the center position where for higher vehicle speeds some overshoot occurs. Although, when friction compensation is used the steering wheel return to its center which was not the case when no return to center assistance was used, compare with figure 6.3.

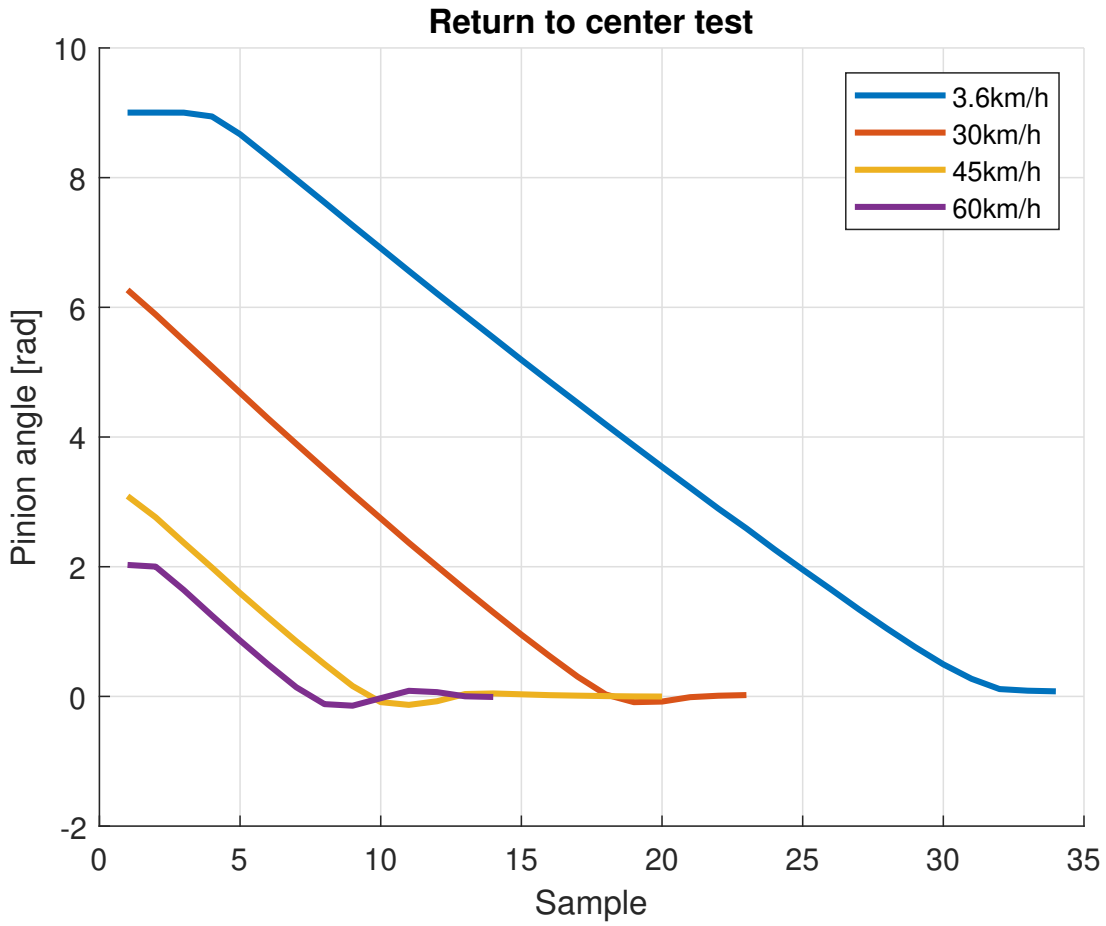

Figure 6.11: *An illustration of how the pinion angle changes during a Return to center test for base torque combined with a return to center assisting friction compensation.*

6.3.2 Return to center assistance by integration

To measure the impact of adding the second method of the return to center feature by adding a torque generated by integrating part depending on the pinion angle to the steering feel model, a Ramp steer test was conducted at three different vehicle speeds, namely 30km/h, 45km/h, and 60km/h. The resulting torque profiles are depicted in Figure 6.12. The reference torque profile can be seen in the figure to deviate from the EPAS measurements, with greater deviations observed at lower vehicle speeds. Specifically for 30km/h, the torque profile is significantly lower up to a pinion angle of 2rad where the deviation starts to increase again. For pinion angles beyond 2rad, the slope gradients differ greatly from the EPAS measurements. At 45 km/h, the reference torque curve closely follows the EPAS measurements up to an approximate pinon angle of $x_2 = 0.5$rad, with a slight decrease of y_2, i.e. the peak torque of the second-degree polynomial, part of the base torque curve. However, the slope gradients were increased for angles above $x_2 = 0.5$rad, resulting in higher torque values. For 60km/h, the reference torque profile resembles the EPAS measurements closely but with a lower torque value throughout. During a loss of grip scenario across all vehicle speeds, the torque profile reaches a non-zero constant torque value, as can be seen in figure 6.12. The estimated FFb actuator torque closely follows the reference torque profile except for being affected by cogging torque, resulting in fluctuations in the torque profile.

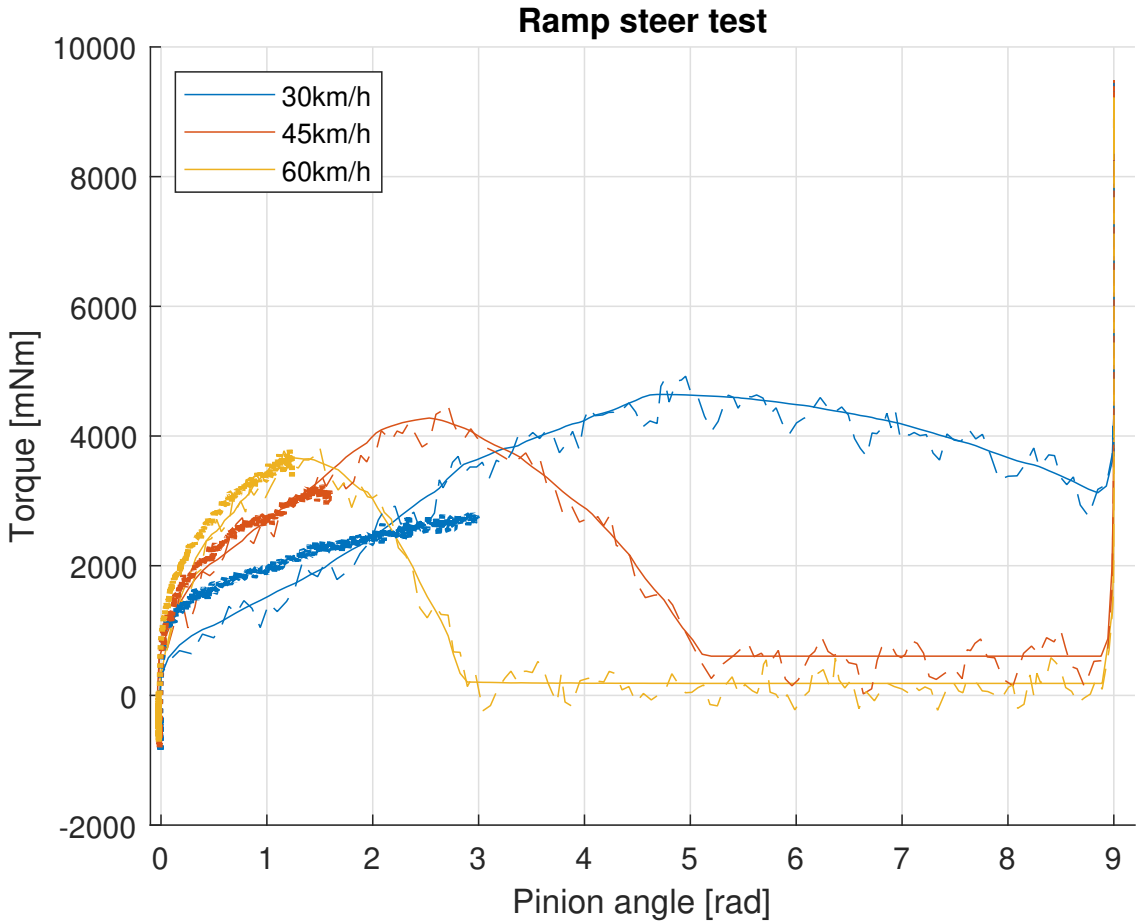

Figure 6.12: *Resulting base torque combined with a return to center assisting integration as a function of pinion angle after performed Ramp steer test. The solid lines are the reference torque generated by the reference generator, the dashed lines are the estimated torque acting on the steering wheel, and the dotted lines are the torque taken from measurement in an EPAS vehicle.*

A Ramp steer test on the steering feel model at a vehicle speed of 3.6km/h for the base torque added with the return to the center integrator was also performed, where the behavior of adding an integrator can be seen more clearly at low vehicle speeds. Figure 6.13 shows the resulting torque profile. The curve initially rapidly

reaches approximately 500mNm. Beyond $x_2 = 0.5$rad, the curve appears to achieve nonlinear behavior until the steering angles surpass 2.8rad, at which the torque curve becomes linear.

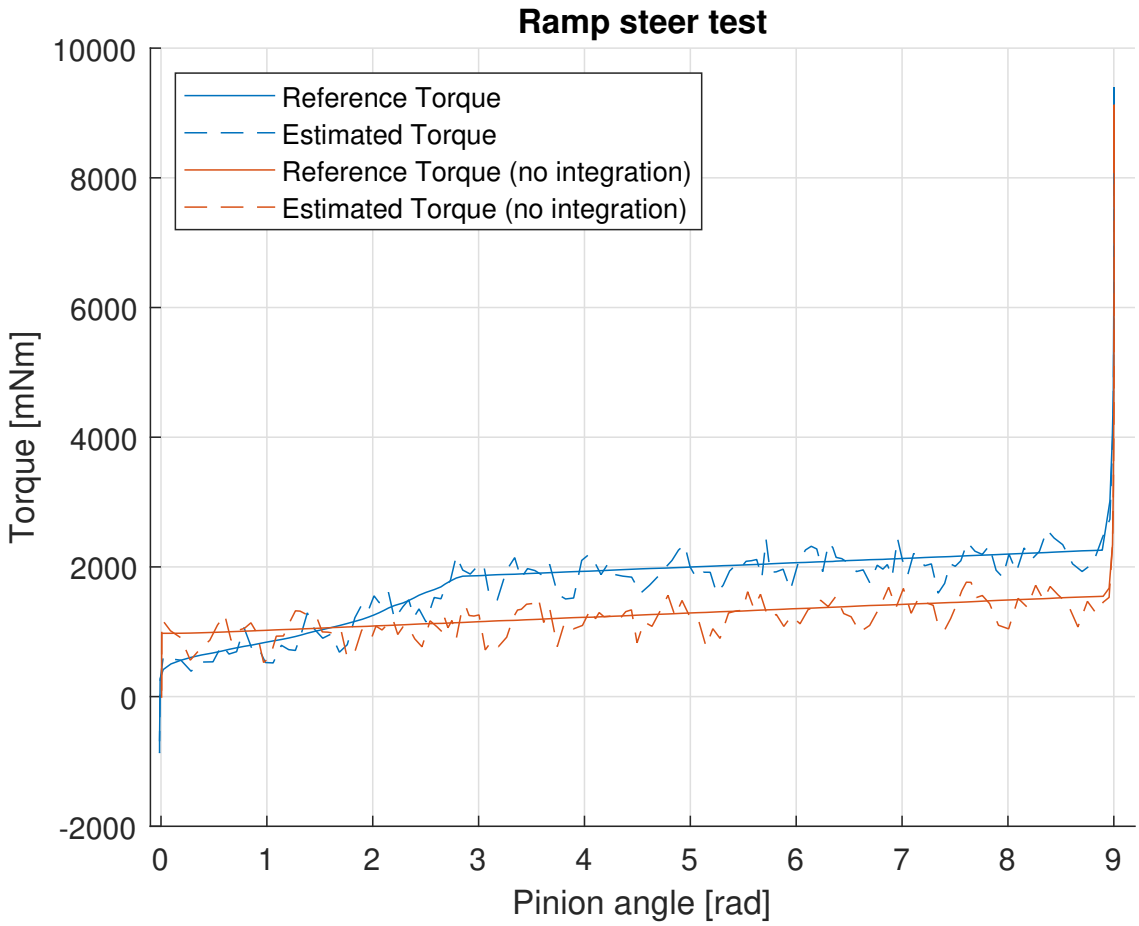

Figure 6.13: *Resulting base torque combined with a return to center assisting integration as a function of pinion angle after performed Ramp steer test. The solid lines are the reference torque generated by the reference generator, and the dashed lines are the estimated torque acting on the steering wheel.*

Figure 6.14 illustrates the results of doing a Weave test with the same setup for the vehicle speeds of 30km/h, 45km/h, and 60km/h. Where the reference torque and estimated torque can be compared to the EPAS measurements. It can be seen that the torque curve when turning away from the center follows the EPAS measurements relatively well for all vehicle speeds if the pinion angle is positive. The torque is lower when turning away from the center when the pinion angle is negative and the characteristics of hysteresis because of the steering wheel being turned towards the center differs from the EPAS measurements. It seems to be some sort of imbalance in the torque generation where the torque curve follows the EPAS measurements if the pinion angle is positive and worse if the pinion angle is negative. For a vehicle speed of 60km/h, it can be clearly seen that the amount of torque when turning toward the center differs more, especially if the pinion angle is negative.

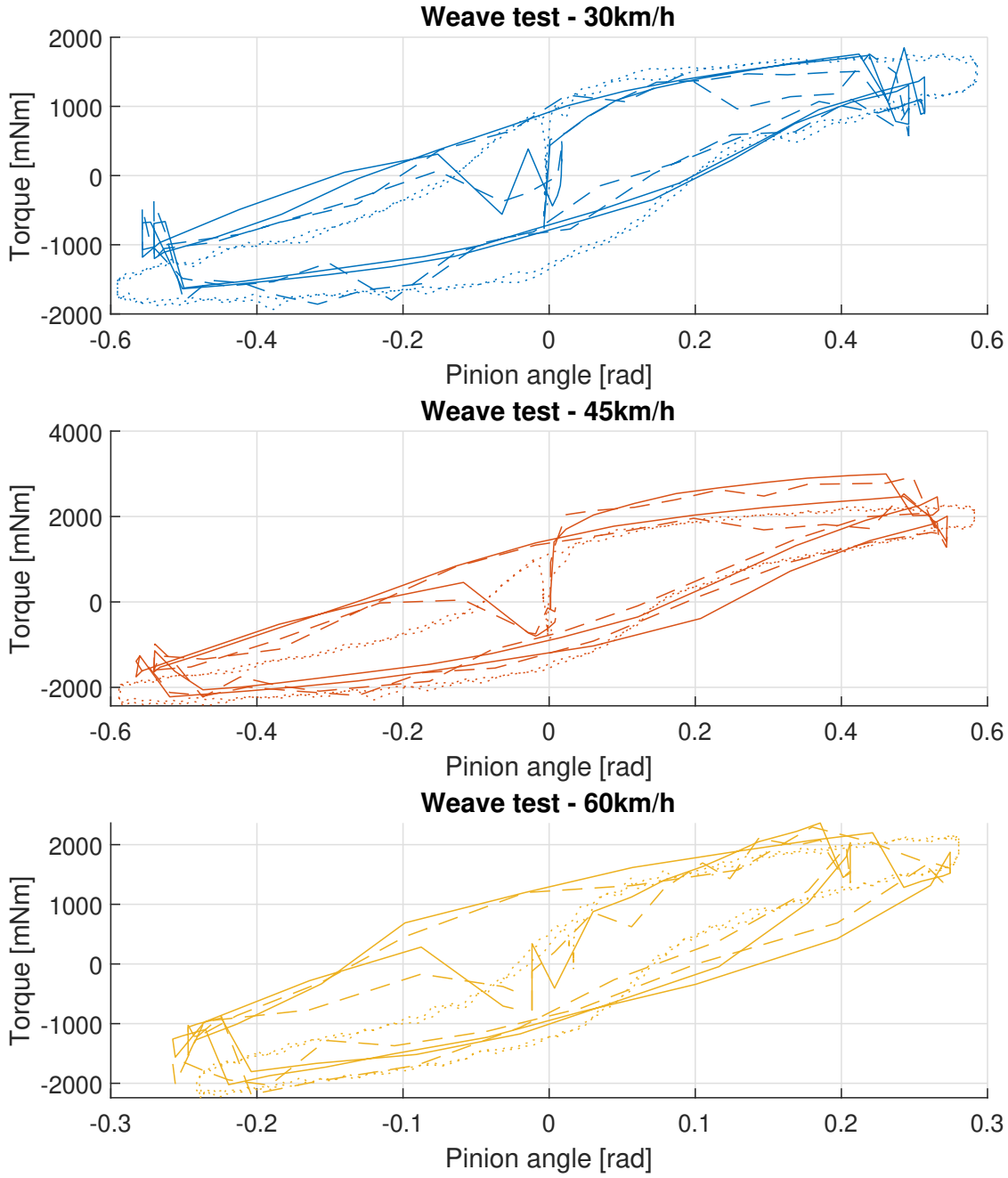

Figure 6.14: *Resulting base torque combined with a return to center assisting integration as a function of pinion angle after performed Weave test. The solid lines are the reference torque generated by the reference generator, the dashed lines are the estimated torque acting on the steering wheel, and the dotted lines are the torque taken from measurement in an EPAS vehicle.*

The results of the Weave test conducted at a vehicle speed of 3.6 km/h are depicted in Figure 6.15 as a comparison with the case without integration. It can be clearly seen that there is no resemblance between the two cases. However the true profile with integration appears to resemble the torque profiles for higher vehicle speeds, compare to figure 6.14.

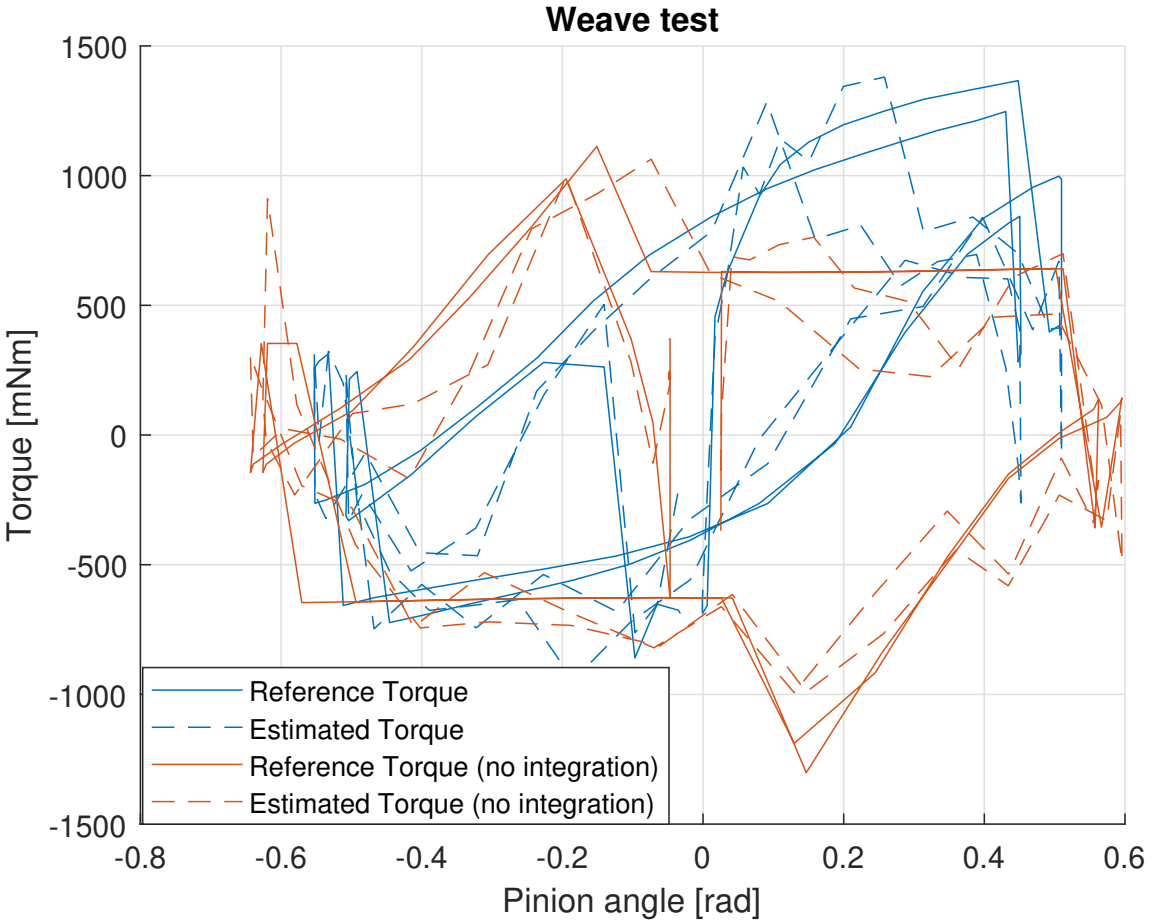

Figure 6.15: *Resulting base torque combined with a return to center assisting integration as a function of pinion angle after performed Weave test. The solid lines are the reference torque generated by the reference generator, and the dashed lines are the estimated torque acting on the steering wheel.*

Figure 6.16 shows the results of a Return to Center test performed at vehicle speeds of 3.6 km/h, 30km/h, 45km/h, and 60km/h. The test reveals that the output of the steering model experiences difficulty in reaching a pinion angle of zero. The algorithm instead overshoots several times before finally reaching it. Each time the curve overshoots, the value remains constant for a brief period. This occurs especially for lower vehicle speeds.

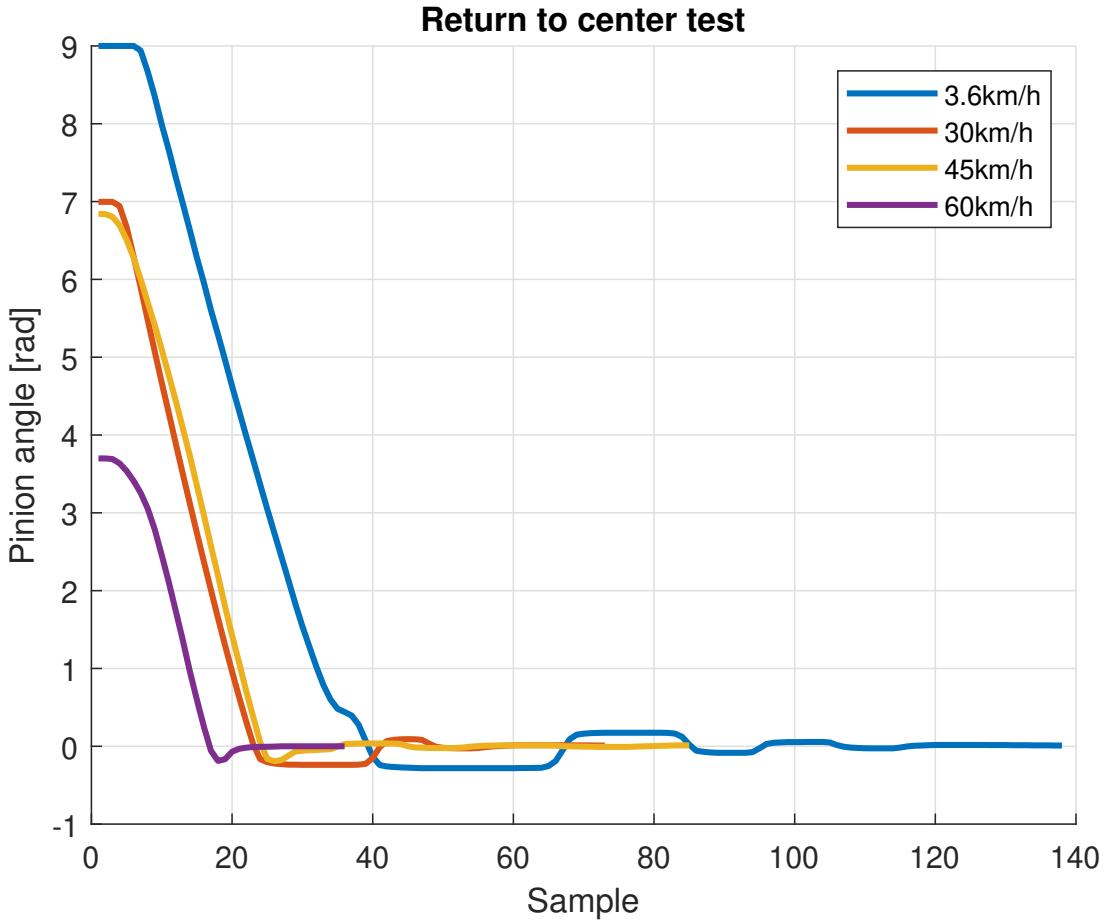

Figure 6.16: *An illustration of how the pinion angle changes during a Return to center test for base torque combined with a return to center assisting integration.*

6.4 Torque at zero velocity

To compare the base torque profile for the steering feel model and EPAS at a vehicle speed of 0 km/h, the following test was performed illustrated in figure 6.17.

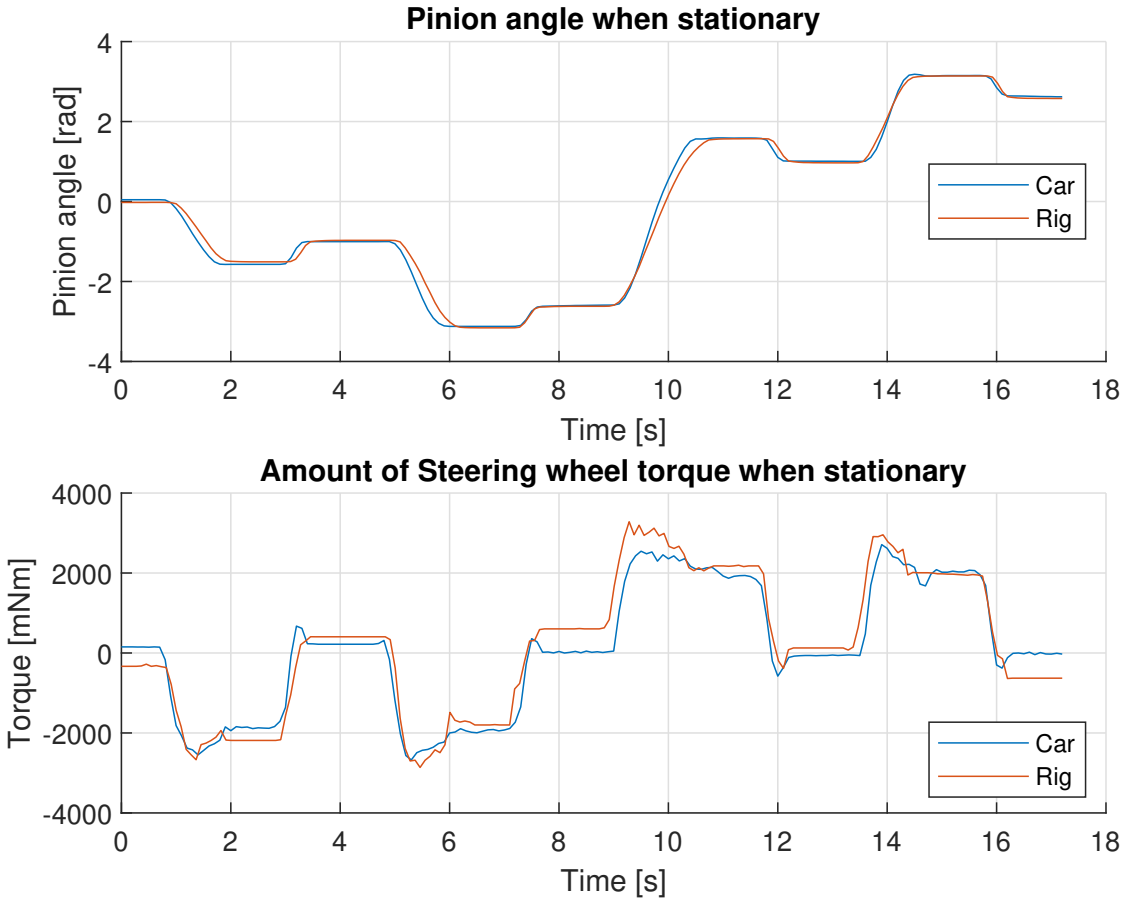

Figure 6.17: *An illustration of pinion angle and torque for the base torque profile for a stationary vehicle.*

As observed in figure 6.17, the steering wheel was turned to 90 degrees, and then the hands were released from the steering wheel. After approximately two seconds, the steering wheel was turned to 180 degrees, and the hands were released from the steering wheel again. Thereafter, the same process was performed but for negative steering wheel positions.

The car measurements were performed in an EPAS vehicle and the steering feel model was performed on the testing rig. The steering feel position curve can be seen to closely follow the EPAS measurements in figure 6.17. When the hands were released, the pinion position was retracted 0.62rad back to the current center position for both tests giving almost identical results. For the torque profile, the steering feel model has similar torque profile characteristics. The torque peaks are reached simultaneously giving an overshoot in torque before converging to a steady value. The peak values are approximately within the range of [2200:3000]mNm and the steady torque values are within [1900:2200] mNm.

6.5 Displacement of zero torque position

By observing figure 6.18, two different torque profiles are shown when a displacement of the zero torque position is moved 1rad in each steering direction. As can be seen in the figure, the difference in the torque profile by adding a displacement is the change of slope gradients of the torque until the position where the loss of traction occurred. The torque profile characteristics for the remaining parts, where the end stop was initiated and the slope between the loss of grip and the end stop remained identical.

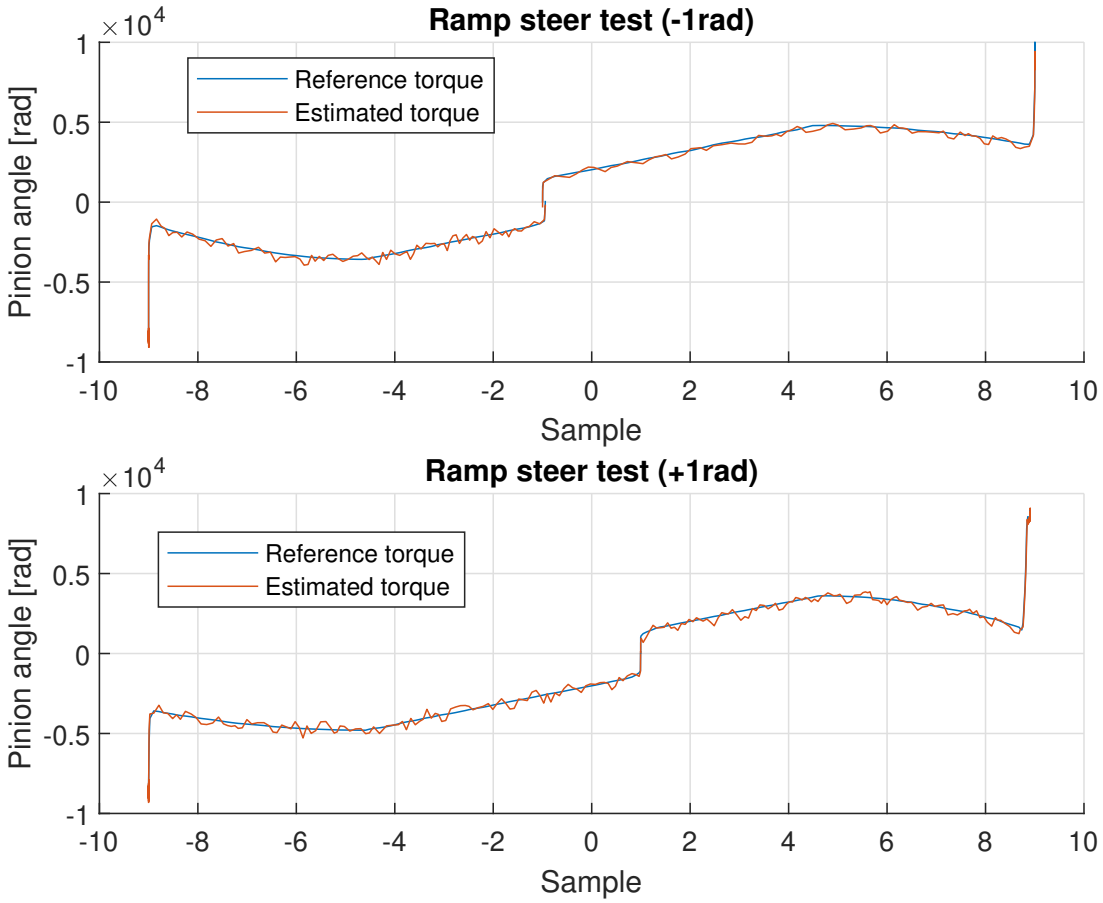

Figure 6.18: *Illustration of a Ramp steer test for both positive and negative pinion angle with a displacement of the zero torque position where the blue lines are the reference torque and the orange lines are the estimated torque.*

A Weave test while adding a displacement of the zero torque position of 1rad to each steering direction was performed and the results can be observed in figure 6.19. The test was performed at a vehicle speed of 30 km/h with no additional damping or return to zero feature added to the steering feel model. It can be seen that the center position was moved to ±1rad by observing the pinion angle of the start and finish positions of the test. However, the torque profile alone is identical to the profile generated by the base torque steering feel model active at a vehicle speed of 30 km/h but shifted ±1rad.

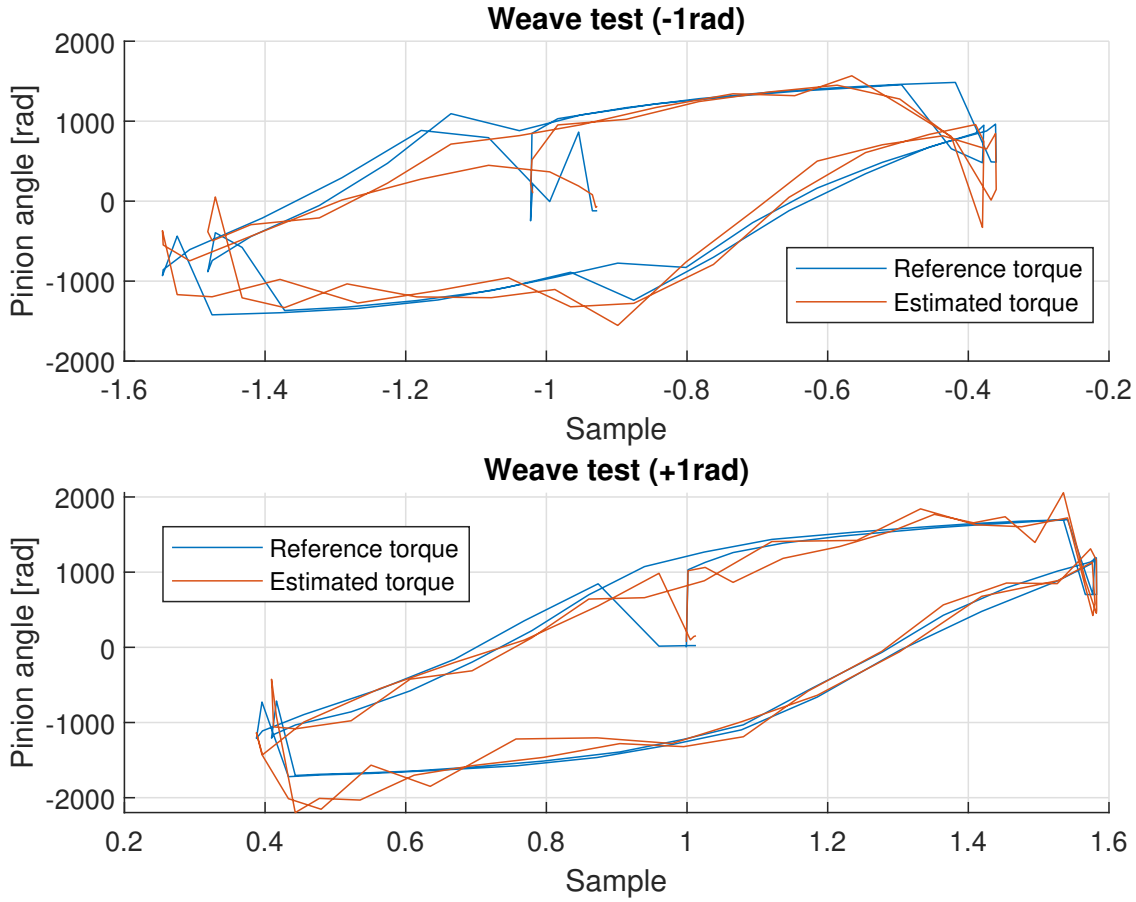

Figure 6.19: *Illustration of a Weave test with a displacement of the zero torque position where the blue lines are the reference torque and the orange lines are the estimated torque.*

Figure 6.20 illustrates the results by performing two Return to center tests, one in each steering direction. The steering feel model was tested at a vehicle speed of 30 km/h with a displacement of the zero torque position of ±1rad and no additional features active. The results were next to symmetrical for both displacements. The direction closest to the displacement of the zero torque position managed to return to the new center position, and the one further away did not manage to return.

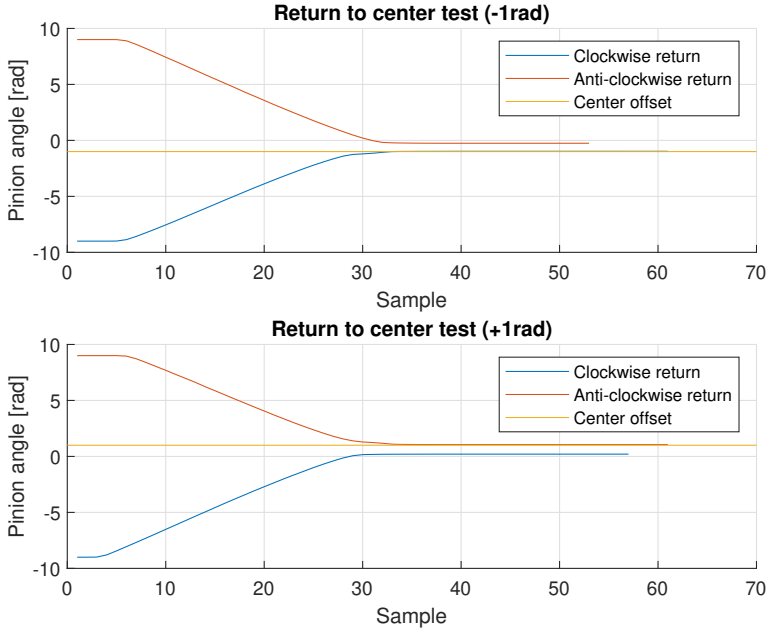

Figure 6.20: *Illustration of a Return to center test with a displacement of the zero torque position where the blue lines are the pinion angle when returning to center with a clockwise rotation, the orange lines are the pinion angle when returning to center with an anti-clockwise rotation, and the yellow lines represent the pinon angle at which the zero torque position is located.*

6.6 Test track

As a final test for evaluating the steering feel model, the steering feel model was implemented into a passenger vehicle with an identical hardware setup as the testing rig. The vehicle was driven around a longer testing track with steep curves and one short track with four tight 90-degree corners. As an objective evaluation of the steering feel model, the vehicle was driven twice around each track, once with the regular EPAS system and once with the SbW system. While doing this the steering wheel torque for the EPAS system and the pinion angle were measured, and the steering wheel torque applied by the FFb actuator torque was estimated. The longer track was driven at approximately 60km/h during the whole lap and the short track was driven at approximately 10km/h.

Figure 6.21 below shows the steering wheel torque and the pinion angle for the two systems in comparison to each other for the long track. As can be seen in the figure is the amount of torque generated by the FFb actuator very similar to the torque in a steering wheel from an EPAS system. Though for two of the curves does is the FFb torque a little lower than for the EPAS system even if the pinion angle for both those curves is very similar.

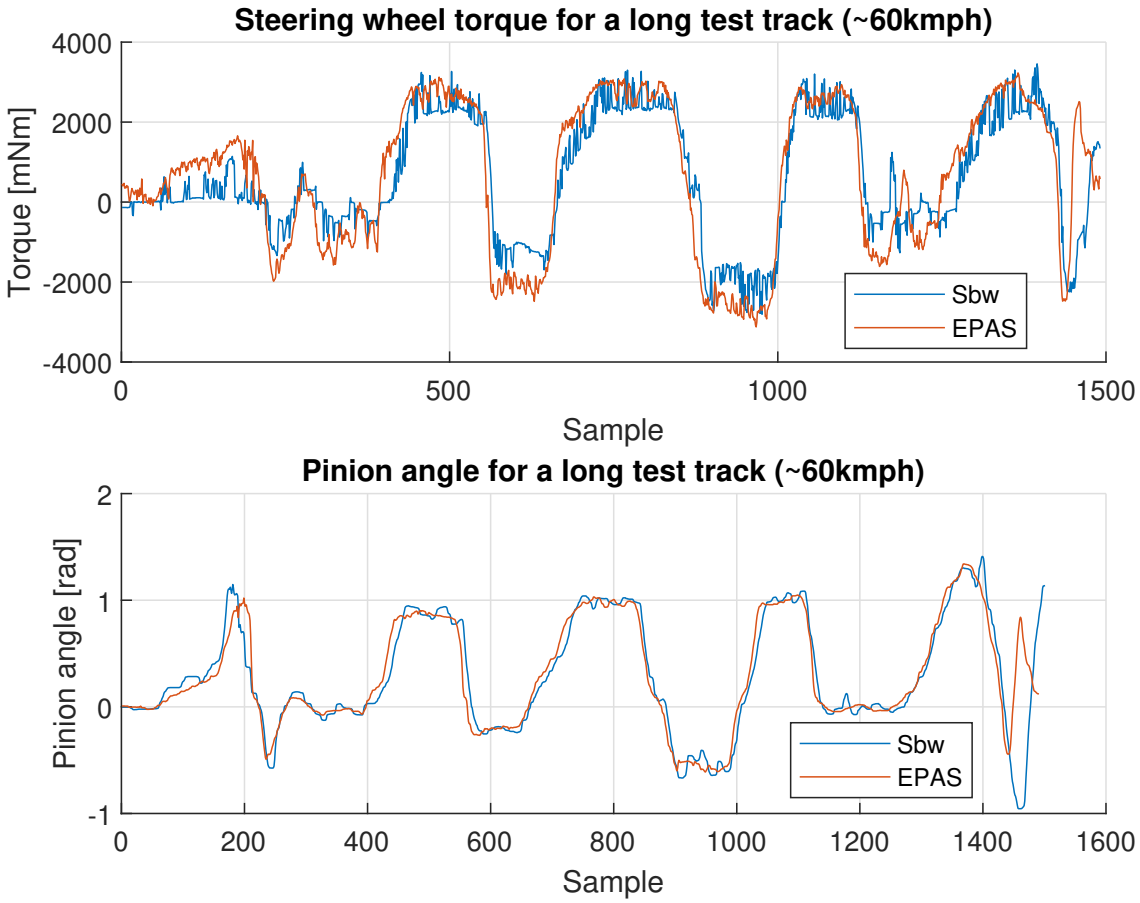

Figure 6.21: *The measured steering wheel torque and measured pinion angle from an EPAS system, and the estimated torque and measured pinion angle from the Sbw system while driving a longer track at approximately 60km/h.*

Figure 6.22 below also shows the steering wheel torque and the pinion angle for both the EPAS and the SbW systems. Here it can be seen that the amount of torque applied from the FFb actuator is very similar to the torque measured in the EPAS system. However, the torque curves do not fully match the whole sequence and this is due to the vehicle not maintaining a constant speed of 10km/h. It can be seen in the pinion angle plot in figure 6.22 that the vehicle was driven a little bit faster while measuring the torque for the EPAS system at

the beginning of the track until the third curve when the vehicle maintained the same speed for both systems.

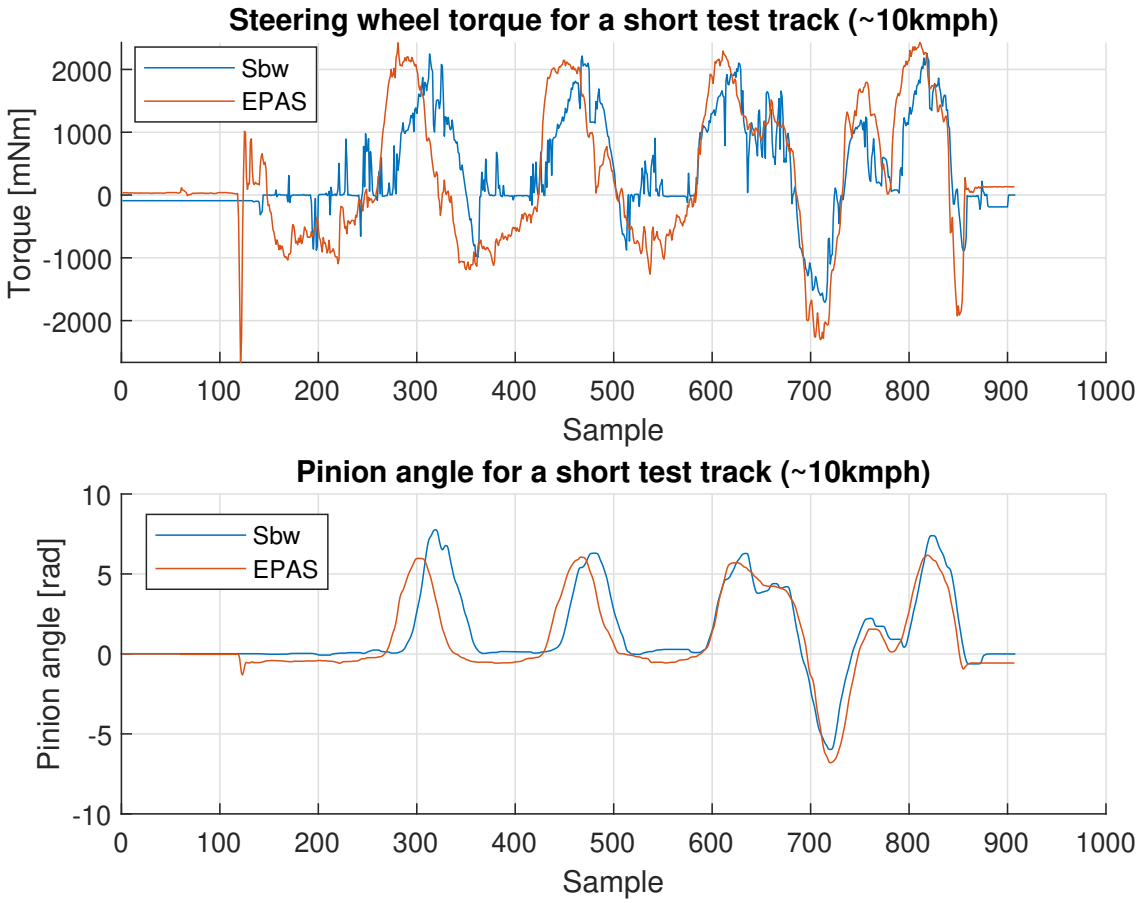

Figure 6.22: *The measured steering wheel torque and measured pinion angle from an EPAS system, and the estimated torque and measured pinion angle from the Sbw system while driving a shorter track at approximately 10km/h.*

6.7 Cogging Torque

A test to evaluate the cogging torque by studying the difference between the torque with and without the integrated cogging compensation for the FFb actuator was performed. The test was executed such that the steering wheel was set to start at five different angles and then slowly started to linearly increase the torque of the FFb actuator until the steering wheel started to move. Thus this test shows approximately the torque required to move the steering wheel at different starting positions and thus the irregularities of the cogging torque. Figure 6.23 below shows the resulting torque curves for the test with and without cogging compensation where the solid lines are the torque estimated by the integrated torque estimator in the FFb actuator, the dashed lines are the reference torque, and the red marker is the point where the steering wheel starts to move.

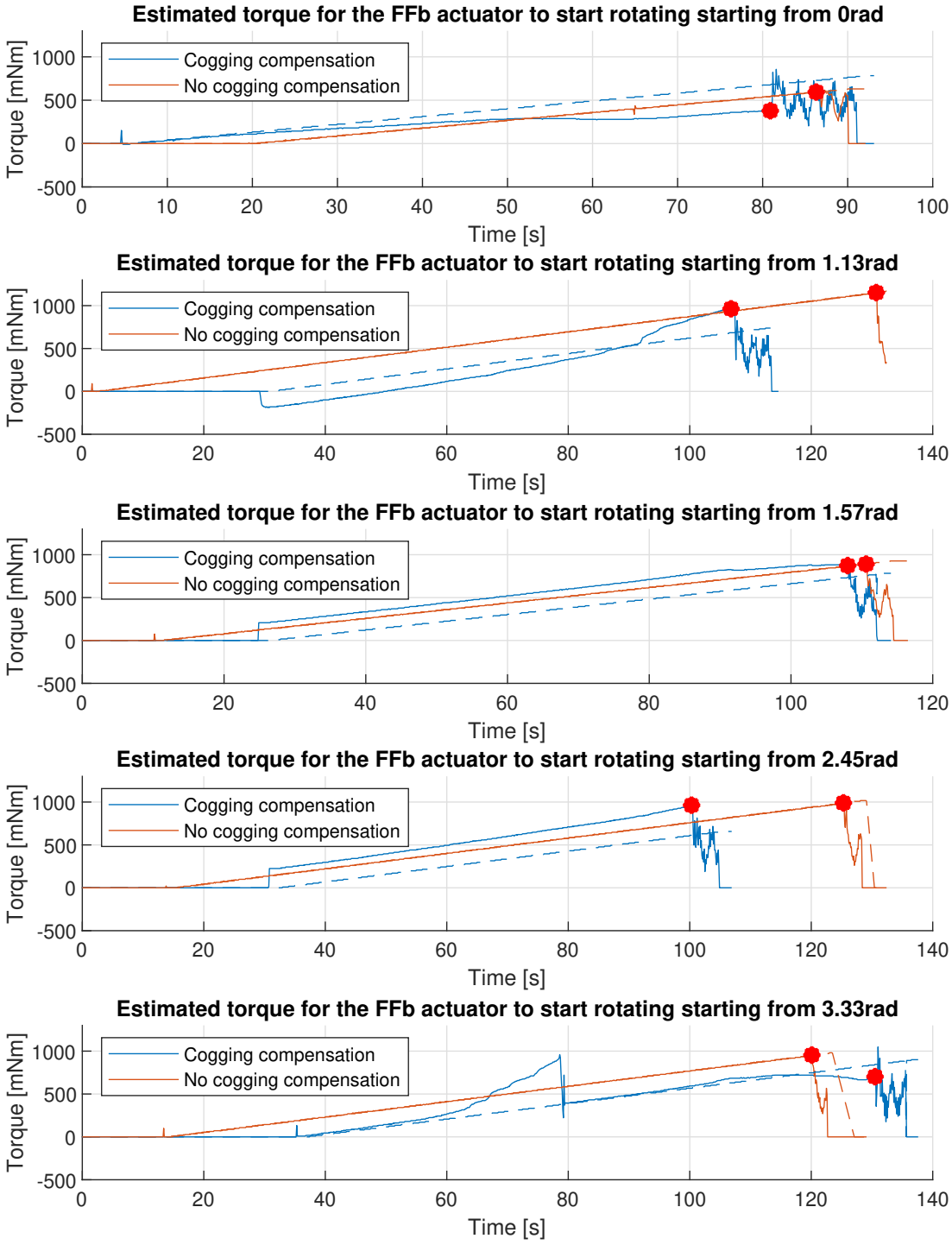

Figure 6.23: *Amount of torque required to move the steering wheel from a stationary position where the solid line is the estimated torque, the dashed line is the reference torque, and the red marker is the point where the steering wheel starts to move.*

The first thing that can be noted from figure 6.23 is that the estimated torque and reference torque for when no cogging compensation is used is almost identical until the point that the steering wheel starts moving. However, when the cogging compensation is activated the estimated torque and reference torque is rarely the same and it seems, depending on the starting position, that the estimated torque initiates at a larger or smaller value than the reference torque indicates that the actuator should have. From the plots when the steering wheel starts at positions 1.13rad and 3.33rad it can be clearly seen that the estimation of the torque might not be 100% correct because of the inconsistent behavior around the times 90s and 80s in the respective plots. It can be seen from all plots that the amount of torque needed to move the steering wheel is larger if no cogging compensation is used if only the estimated torque is taken into consideration. According to the first plot where the starting position is 0rad the reference torque is larger before the steering wheel starts to move for the case where cogging compensation is used than when no cogging compensation is used.

7 Discussion

The steering feel model was effectively developed to emulate the forces that strive for the steering wheel to be centered in an EPAS system, achieving successful results. However, certain additional forces that contribute to a good steering feel, such as steering vibrations caused by road surface roughness, were not incorporated into the model. Thus, the base torque was derived from the observed behavior of the aligning torque and system friction torque, as indicated by the EPAS measurements, which generated satisfactory outcomes. Developing a base torque profile for turning away from the center position was relatively straightforward since the steering feel was the primary consideration. However, when turning towards the center, additional factors had to be taken into account, namely the active return and the desired torque profile hysteresis. As a result, while the base torque profile closely matched the EPAS measurements for steering away from the center position, it differed significantly for the opposite direction. To ensure good steering feel with the available hardware setup, it was necessary to fine-tune the steering feel model. This fine-tuning process revealed an increasing discrepancy in the hysteresis compared to the EPAS measurements, particularly noticeable at higher vehicle speeds. This discrepancy can be attributed to the tough tuning conditions given by the significant fluctuations in the cogging torque combined with the system friction. The development of hysteresis followed a consistent methodology across all vehicle speeds. However, compared to the steering feel model, the hysteresis for the EPAS measurements appeared to decrease for low angles at elevated vehicle speeds.

Subjectively, the difference in hysteresis observed in practice contributed to desirable steering feel while implemented on the hardware available. The presence of a larger hysteresis implies that the steering wheel faces challenges in returning to the center position due to the combined effect of system friction and cogging torque. However, the higher magnitude of the torque profile at elevated vehicle speeds led to the steering wheel overshooting during the return to the center position. The on-center damping effectively mitigated the overshoot, ensuring a smooth convergence to zero creating a pleasant steering feel. Nonetheless, the presence of cogging torque significantly influenced the overall feel of maneuvering the steering wheel, especially at small angles as the steering wheel frequently got caught on large cogs at vehicle speeds below 30 km/h.

For a scenario when the vehicle is stationary, the steering feel model produces a base torque profile that closely resembles the torque profile generated by a vehicle integrated with EPAS. While maneuvering the steering wheel, the torque profile for both scenarios was next to identical, subjectively resulting in a good steering feel difficult to distinguish from one another.

The combined effects of the system friction and the cogging torque led the steering feel model to face challenges in returning the steering wheel to the center position. To compensate, two methods were explored to incorporate an active return functionality into the model. The first method is based on adding a steering direction-based constant to y_2 to neutralize the external forces not included in the steering feel model. This method successfully brought the steering wheel back to the center position successfully at all vehicle speeds. However, it led to a significant change in the torque profile. When steering toward the center, the torque increased considerably compared to steering away from it. At low vehicle speeds, steering away from the center position resulted in minimal torque resistance, which was deemed undesirable. The same principle was applied while steering away. In general, compensating for the system friction and the cogging torque, required a larger compensation than desired. Adding friction compensation generated a torque profile much too different from the EPAS measurements and subjectively resulted in an unpleasant steering feel with low overall resistance. The second method, which instead utilized an integral part in the model, also managed to bring the steering wheel back to the center position consistently. Although, it led to the steering wheel easily getting caught on large cogs near the center before finally becoming completely centered. The torque profile while integrating an integral part to the model, deviated considerably from the EPAS measurements due to the non-linear slope before reaching the maximal torque threshold generated by the integral part, followed by a constant slope thereafter. Since the effects of system torque combined with fluctuating cogging torque, developing a fully functional integral part with a smooth convergence to the center position was considered difficult. Due to the cogging torque, in order to move the steering wheel while getting caught on a cog, the integrator had to be aggressively tuned with a high maximal torque value. Subjectively, similar to the first method, this led to an unsatisfactory steering feel.

The steering feel model was effectively designed to incorporate a decrease in the torque profile as the grip between the tires and the road surface declines. Since there were no available EPAS measurements depicting an actual torque profile for an understeer scenario, a straightforward design based on a second-degree polynomial was implemented to develop the torque profile for such a scenario. The primary objective was to subjectively be able to detect the decrease in grip while maneuvering the steering wheel, a factor that could be easily

determined. However, the torque profile will continually reach a threshold value. This threshold value can be adjusted to achieve a more realistic torque profile during understeer if desired.

In the scenario where the vehicle experiences oversteer instead of understeer, the steering feel model incorporates the option to modify the displacement of the zero torque position. However, no specific solution has been developed to address how the torque profile should adjust in the case of a loss of traction due to oversteering. Nevertheless, the torque profile is adjusted based on the displacement when no oversteer is present. In this case, the torque profile remains consistent for steering angles beyond the point of traction loss in an understeer scenario. While adding a displacement, the torque profile closely resembles the base torque profile combined with the on-center damping, providing a natural and satisfying steering feel in both steering directions. At lower vehicle speeds, the steering wheel faces challenges in returning to the displaced center position in the direction with a longer travel distance. Consequently, the steering wheel struggles in returning to the center position at higher vehicle speeds when compared to no displacement added.

Additionally, the model was effectively designed to compensate for the lack of mechanical limitations of the steering wheel by incorporating a rapid increase in the torque profile for steering angles beyond a specified interval. This solution followed a non-linear spring-damper model to define the behavior within this range. The main objective was to develop a torque profile that would undoubtedly signal the driver when the maximum steering angle had been reached. Subjectively, deliberately attempting to turn the steering wheel beyond its limits is not easily achievable. The torque profile's distinctive increase serves as a clear indication, while also ensuring that the FFb actuator does not undergo excessive strain from excessively high torque values. The steering feel remains appropriately balanced, with sufficient resistance when steering against it with slight spring-like behavior, indicating a robust damper capable of effectively dampening the high torque values at the end-stop of the torque profile. Similarly, when an obstacle is detected because of a difference between the pinion angle and the steering wheel angle the same torque profile is generated to signal the driver that an obstacle has been struck while turning. However, the solution of detecting an obstacle is not optimal. Since the possibility of the steering wheel and steering rack not being synchronized because of the limitations of the steering rack actuator the steering feel model might think that an obstacle has been struck. This means that the steering feel model will generate the End-stop torque curve for an obstacle when no obstacle has been struck in reality.

To maintain synchronization between the steering rack and steering wheel, an attempt was made to integrate a feature that limits the angular velocity of the steering wheel to match the maximum velocity of the steering rack. This was achieved by introducing additional torque feedback. Two methods were explored to find a solution, but both methods proved unsuccessful and resulted in an unsatisfactory steering feel. The first method, based on a PI-controller, did not manage to limit the angular velocity to never exceed the maximum angular velocity. The controller also causes a jagged-like steering feel, which was deemed undesirable. The second method, utilizing a hyperbolic function damper, also prevented the angular velocity from surpassing the maximum velocity. Although, in order to achieve a satisfactory steering feel, the active range of the damper needed to be too large. As a result, the torque profile was excessively dampened for steering angles that should not be dampened, significantly affecting the steering feel.

The cogging torque appeared as the primary factor impacting the overall performance of the steering feel model in a negative manner. It constantly affected the maneuvering experience of the steering wheel and while unhanded prevented the wheel from returning to the center position, despite the reference torque generated by the model should have been sufficient. The model was required to produce a substantial torque output to move the steering wheel from a standstill to overcome the resistance encountered when stuck in a cog. Consequently, the high torque values and fluctuations of the cogging torque significantly influenced the development of each feature since careful consideration had to be given, to neutralize the effects of cogging torque during implementation.

Besides the cogging torque, another factor that impacts the overall performance of the steering feel model in a negative manner is the current steering rack actuator. Since the maximum angular velocity of the pinion in the steering rack is 6rad/s it causes aynchronization between the steering wheel and the steering rack when turning the steering wheel faster than 6rad/s. The asynchronization is even worse with a steering ratio greater than 1:1. For example if the steering ratio between the steering wheel and the pinion in the steering rack is 2:1, then a 360 deg turn of the steering wheel corresponds to 180 deg of the pinion which means that the steering wheel can not be rotated faster than 3rad/s to cause asynchronization. Future work would thus include either replacing the steering rack actuator or investigating if it is possible to increase the maximum angular velocity of the actuator. If this could be achieved a need for an angular velocity limiter would not exist which would positively affect the steering feel such that no additional torque generation affects the overall steering feel.

It has been noted in previous chapters that there are alternative approaches to generating torque feedback.

As discussed in chapter 3 the torque feedback is generated by physicalities in the mechanical steering system. Using mathematical models it is possible to model these physicalities to generate the torque feedback. Though there are more physicalities acting on the system than just the aligning torque and friction torque. The physicalities of the tires are another contribution to the steering feel. Where the physics of tires is a large and active research field where a number of different mathematical models of tires have been developed. The problem with using mathematical models for real-time physicalities is that the models are only approximations of the real thing and thus do not represent the true physicality. If enough well-represented models of the different physicalities acting on the real steering system were to be gathered to generate a relatively accurate torque feedback this would represent the true torque feedback without any assisting power steering. Hence is the need for a boost curve that would represent the power steering also needed to achieve a steering feel similar to the EPAS system. This boost curve is thus not model-based and is a fully tunable parameter of the steering feel similar to the approach made for this project to achieve the complete steering feel. Using a model-based reference generator for the torque feedback would not take other external forces that might give necessary information to the driver such as curbs, rocks, potholes, etc. This also applies to the approach made in this project.

Another alternative approach to generating a satisfying steering feel is by taking all forces generating the torque feedback into consideration. This can be done by using a rack force observer, see [6] for an example. A rack force observer is an observer that estimated the force acting upon the steering rack which in return generates the torque feedback in the steering wheel. By using an observer all forces that might affect the steering system can be estimated and thus be generated as torque feedback to the driver. This gives full transparency between the driver and the road which is not possible through the approach in this project or the model-based approach. However, an observer is still model-based such that a prediction has to be made but is then updated through real-time measurements to acquire a good estimation. Full transparency between the driver and the road can also be seen as a downside since this means that all information from the road will be transmitted to the driver via torque feedback. Some information is wished to be filtered out to achieve a fully satisfying steering feel, such as steering wheel movement on a rutted road or steering vibrations caused by brake judder, see [14].

All methods possible to generate a satisfying steering feel come with both pros and cons. As discussed above the approach in this project does not depend on the physicalities of the system and how these affect the steering feel. It also does not depend on any boost curve that is needed to be tuned for the power steering. The downside of this approach is the loss of full transparency between the driver and the road since the torque feedback generated by the approach of this project is for the "ideal case of driving" where no additional external forces act upon the system that might be useful for the driver to acknowledge such as steering vibrations caused by the road surface roughness. Whereas by using the model-based approach the physicalities of the system and the boost curve have to be taken into consideration and the full transparency is lost. For the rack force observer case, some type of modeling and boost curve also have to be used but the full transparency between the driver and the road can thus be achieved. The downside with the observer is though how the information not wanted is supposed to be filtered out.

As for the subjective evaluation of the steering feel what could have been seen as a problem and a limitation was that the steering wheel for the SbW system in the testing vehicle was mounted on the right side of the vehicle. This can be very unfamiliar for a driver that has solely driven a vehicle with the steering wheel on the left side. Subjectively speaking, having the steering wheel on the left side could be a great advantage for the driver to get a better sense of the steering feel.

8 Conclusion

In conclusion, the developed steering feel model successfully incorporates the selected set of features and provides torque feedback to the steering wheel during normal driving conditions. The model includes a set of tunable variables that adjust the torque profile accordingly. It assumes a given variable steering ratio and generates the desired outcome based on that. The results suggest an effective development of the base torque combined with on-center damping, loss of traction torque profile, end-stop, displacement of the zero torque position, and a torque profile at zero vehicle speeds. These features were assessed both in unity and individually, and subjective evaluations of the steering feel were conducted. However, it is worth noting that the tests were performed manually by human hands and may not have been executed optimally. Overall, the tuned steering feel model provided satisfactory steering feel for both real-life testing on the testing rig and in the testing car. Although, it is important to acknowledge that optimal end results could not be achieved, primarily due to the influence of the cogging torque. The return to zero and angular velocity limiter features showed less successful results based on the performed tests and were not included in the final version of the model while implemented in the test car for subjective evaluation.

As previously introduced in earlier chapters, using EPAS measurements is not the only approach to generating torque feedback. It can also be achieved by utilizing mathematical models to model the physicalities affecting the mechanical steering system during normal driving conditions and combined with boost curves the desired steering feel can be achieved. Another alternative would be to implement a rack force observer but indifferent to the previous methods would be that all forces acting upon the steering system at all times affect the torque feedback, not just the forces acting upon the system during normal driving conditions. However, a model-based approach or a rack force observer does not guarantee the same steering feel as that of an EPAS system in the same way as the approach in this project. By using EPAS measurements the steering feel can be almost copied exactly after the torque feedback in the steering wheel without taking any physicalities or boost curves into consideration.

The overall experience of this project has been great and it has been insightful to apply knowledge in practice. It has been very interesting to apply our knowledge in the automotive industry and learn more about vehicle dynamics and how so many small parts of one system can make a difference in the performance of the system as a whole. A lot of new useful information has been collected during this project which will be used in the future.

9 Future work

Future work is required to improve the overall quality of the product where the first step would be to investigate what kind of actuator would fit best as an FFb actuator such that performance meets the criteria needed for a satisfying steering feel. These criteria include for example no cogging torque such that the steering is smooth at all times, not too big in size such that it fits behind the steering wheel and does not weigh too much, and enough torque such that the maximum torque needed for example the End-stop can be generated. As of right now, the cogging torque is the problem with the current FFb actuator which subjectively is a significant problem since it does not generate a perfectly smooth steering feel.

Since the torque profile is not accurate for all vehicle speeds a more in-depth investigation of the hysteresis has to be done. As of right now, the torque generation causing the hysteresis does not resemble the hysteresis of the real torque curves for all vehicle speeds. Thus it needs to be investigated what causes the hysteresis to get a better understanding of how it can be emulated for all vehicle speeds. More Weave tests for different vehicle speeds could be the solution to get a better understanding of how the hysteresis is affected by the increase in vehicle speed. This would probably also benefit greatly from a better-performing FFb actuator since the cogging torque negatively affects the measurements of the torque during testing and evaluation. Maybe only replacing the FFb actuator would give more satisfying results of the hysteresis. A different problem currently present in the steering feel model is that the moment when the steering wheel changes the direction of travel the torque is decreased with 1000mNm and then almost instantly increased with 500mNm when it should in reality decreases directly with 500mNm. Subjectively it is difficult to acknowledge that this happens but it is still a problem that needs to be fixed in the future.

Future work is required with the implementation of the frictional damping using the tanh function since figure 4.3 shows that there is a drop in base torque at the moment of change in direction which is not the case for the torque feedback in a conventional steering system.

The current method of incorporating the feeling of understeer in the system needs future work. The torque curve for the understeer needs further investigation into how the torque decreases with the loss of grip in reality. As of right now, the torque decreases as a second-degree polynomial which has not been confirmed with any real data of vehicles losing grip. The calculation of the angle at which the grip starts to decrease also needs to be further investigated since the current computation is heavily simplified and assumes constant friction between the tires and the road. This is of course not the case in reality. Further work on a method that better corresponds to reality to calculate the steering angle at which the grip starts to decrease is thus also needed. A better method for calculating the angle at which all grip has been lost is also needed in the future.

Future work regarding the oversteer is also needed, a concept that the zero torque position can be moved was implemented in this project thus demonstrating how the steering perceives in an oversteer scenario. A method for how the zero torque position is moved during an oversteer needs to be developed such that the correct zero torque position is used when in an oversteering scenario. A method for when the vehicle starts to oversteer also needs to be developed such that steering feel software knows when to move the zero torque position. The displacement of the zero torque position does not need to be solely used to emulate oversteer but it can also be used for lane-keep assistance. The zero torque position is thus moved to turn the wheels such that the vehicle is kept between the lines of the road. This also needs further work to be implemented and used in reality. Lane-keep assistance is already something implemented in many vehicles today and might not need to be developed from scratch to acquire a working product.

Another problem currently existing within the steering feel model is that the zero torque position when the vehicle is stationary is saved after the vehicle starts to move and when the vehicle becomes stationary again the steering wheel rotates to the saved zero torque position if no hands are on the steering wheel. A method for specifying the zero torque position to be e.g. the last known steering wheel position when the vehicle becomes stationary after having been moved has to be developed. Such that the torque profile for a stationary vehicle is correct for all cases.

References

[1] *CANoe. Product Information*. Version 6.5. VECTOR, 2022. URL: https://cdn.vector.com/cms/content/products/canoe/canoe/docs/Product%20Informations/CANoe_ProductInformation_EN.pdf.

[2] D. Cao et al. Study on Low-Speed Steering Resistance Torque of Vehicles Considering Friction between Tire and Pavement. *Applied Sciences* **9**.5 (2019). ISSN: 2076-3417. DOI: 10.3390/app9051015. URL: https://www.mdpi.com/2076-3417/9/5/1015.

[3] *CAPL Used With CANoe And CANalyzer*. 2023. URL: https://www.vector.com/us/en/know-how/capl/#.

[4] T. Chugh et al. "Comparison of Steering Feel Control Strategies in Electric Power Assisted Steering". *14th International Symposium on Advanced Vehicle Control (AVEC 2018)*. 2018.

[5] T. Chugh et al. "Design of Haptic Feedback Control for Steer-by-Wire". *2018 21st International Conference on Intelligent Transportation Systems (ITSC)*. 2018, pp. 1737–1744. DOI: 10.1109/ITSC.2018.8569795.

[6] T. Chugh et al. Steering Feedback Transparency Using Rack Force Observer. *IEEE/ASME Transactions on Mechatronics* **27**.5 (2022), 3853–3864. DOI: 10.1109/TMECH.2022.3144245.

[7] *ECU Designing and Testing using National Instruments Products*. 2009. URL: https://web.archive.org/web/20131221083019/http://www.ni.com/white-paper/3312/en/.

[8] H. Fahami, H. Zamzuri, and S. Mazlan. Development of Estimation Force Feedback Torque Control Algorithm for Driver Steering Feel in Vehicle Steer by Wire System: Hardware in the Loop. *International Journal of Vehicular Technology* **2015** (May 2015), 1–17. DOI: 10.1155/2015/314597.

[9] J. Iqbal et al. Adaptive Global Fast Sliding Mode Control for Steer-by-Wire System Road Vehicles. *Applied Sciences* **7** (July 2017), 738. DOI: 10.3390/app7070738.

[10] ISO Central Secretary. *Road vehicles — Test method for the quantification of on-centre handling — Part 1: Weave test*. en. Standard ISO 13674-1:2010. Geneva, CH: International Organization for Standardization, 2010. URL: https://www.iso.org/standard/54302.html.

[11] O. Jonson and E. Enders. "Correlation Work on Shaker Rig Tests and Simulations – An investigation of damper, bushing, friction and tire modeling with respect to vertical vibration insulation". PhD thesis. July 2016. DOI: 10.13140/RG.2.2.11494.52802.

[12] N. Levin et al. Methods to Reduce the Cogging Torque in Permanent Magnet Synchronous Machines. *Elektronika ir Elektrotechnika* **19**.1 (Jan. 2013), 23–26. DOI: 10.5755/j01.eee.19.1.3248. URL: https://eejournal.ktu.lt/index.php/elt/article/view/3248.

[13] Z. Lijun, M. Dejian, and C. Gang. *Noise, Vibrations and Harshness of Electric and Hybrid Vehicles*. SAE International, 2021. ISBN: 978-0-7680-9966-9.

[14] K. Shibata et al. Development of steer-by-Wire System that Assumes Operation Without Changing Grip. *chassis.tech* (2022).

[15] T. Srisiriwanna and M. Konghirun. "A study of cogging torque reduction methods in brushless dc motor". *2012 9th International Conference on Electrical Engineering/Electronics, Computer, Telecommunications and Information Technology*. 2012, pp. 1–4. DOI: 10.1109/ECTICon.2012.6254191.

[16] *VN8900 Interface Family Manual*. Version 6.6. VECTOR, 2022. URL: https://cdn.vector.com/cms/content/products/VN89xx/docs/VN8900_Manual_EN.pdf.

[17] *What is a worm gear*. 2021. URL: https://khkgears.net/new/worm_gear.html.

[18] H. Zhu, W. Zhu, and W. Fan. Dynamic modeling, simulation and experiment of power transmission belt drives: A systematic review. *Journal of Sound and Vibration* **491** (2021), 115759. ISSN: 0022-460X. DOI: https://doi.org/10.1016/j.jsv.2020.115759. URL: https://www.sciencedirect.com/science/article/pii/S0022460X2030585X.

DEPARTMENT OF MECHANICS AND MARITIME SCIENCES
DIVISION OF VEHICLE ENGINEERING AND AUTONOMOUS SYSTEMS
CHALMERS UNIVERSITY OF TECHNOLOGY
Gothenburg, Sweden 2023

CHALMERS
UNIVERSITY OF TECHNOLOGY